energies

Review

A Review of Pile Foundations in Viscoelastic Medium: Dynamic Analysis and Wave Propagation Modeling

Wenbing Wu and Yunpeng Zhang *

Faculty of Engineering, China University of Geosciences, Wuhan 430074, China
* Correspondence: zypsky@cug.edu.cn

Abstract: The dynamic viscoelastic theory of soil–pile interaction dominates the initial impedance calculation during the pile dynamic design and analysis. Further, it provides a firm theoretical ground for the wave propagation simulation, which could be the basis of seismic analysis and some geotechnical testing approaches. This review traces the development history and key findings of viscoelastic soil–pile interaction theory and expounds on the advantages and limitations of various theoretical advances in terms of dynamic design and wave propagation modeling. The review consists of three sub-divisions, which are the longitudinal, horizontal, and torsional viscoelastic soil-pile theories. The development and implement of multi-phase soil constitutive equations, multi-dimensional soil–pile interaction modeling methods, pile–soil–pile mutual interactions in pile groups, and the fluid–structure interaction problems in offshore piles are especially remarked and concluded. Finally, the shortcomings and deficiencies of the present development are pointed out with a view to addressing them in the future.

Keywords: pile; dynamic analysis; energy engineering; dimensional effect; soil–pile interaction; integrity test

Citation: Wu, W.; Zhang, Y. A Review of Pile Foundations in Viscoelastic Medium: Dynamic Analysis and Wave Propagation Modeling. *Energies* **2022**, *15*, 9432. https://doi.org/10.3390/en15249432

Academic Editor: Marco Fossa

Received: 7 November 2022
Accepted: 10 December 2022
Published: 13 December 2022

1. Introduction

Access to energy depends a lot on the construction of energy infrastructures. For instance, the utilization of water conservancy resources requires the construction of reservoirs and hydropower stations [1]; the exploitation of natural gas or geothermal resources involves the construction of risers and pipelines [2,3]; the utilization of wind resources depends on the installation of wind turbines [4–7], etc. Hence, the discipline of geotechnics has been closely related to energy science. The pile foundation is the most popular foundation to support energy superstructures due to its high dynamic load capacity [8,9]. Dynamic capacity or impedance is a primary consideration for the design of foundations supporting energy structures due to the fact that the production and transition of energy usually generate dynamic loads. Considering that the soil deformation is strongly nonlinear and often related to stress paths, a large amount of cumulative deformation is prone to occur if the plastic deformation of soil is permitted [10–12]. The plasticity of soils in recent years has not only been investigated in detail [13] but has also been analyzed in a deterministic and stochastic way [14]. Hence, for most energy structures, the allowable ultimate deformation of the foundation is small and still in the range of elasticity. For instance, the permissible pile head deflection is only 0.5 degrees for monopiles used as the foundation for offshore wind turbines [15]. As a result, the viscoelastic theory is essential and efficient for dynamic pile–soil interaction problems. From the aspect of vibration forms, the viscoelastic pile–soil interaction theory can be divided into three categories, which are longitudinal, horizontal, and torsional vibrations. This paper presents a state-of-the-art review of dynamic viscoelastic pile–soil interaction theories.

2. Longitudinal Dynamic Analysis and Wave Theory

2.1. General Progress in the Longitudinal Soil–Pile Dynamic Interaction Modeling

The longitudinal dynamic analysis of pile foundations is the most developed branch of the topic, compared to the horizontal and torsional ones. This can be attributed to the most prevalent nature of longitudinal vibration in practice. The earliest paper traced back to rigorously discussing the dynamic interaction of footings and soil under longitudinal vibrations comes from Baranov [16], who idealized the soil as a two-dimensional homogeneous medium; however, although Baranov's solution is still in linear elasticity, its sophistication in mathematical derivation limits its accessibility to practicing engineers. Before Baranov's work, a more straightforward and efficient method based on the Winkler foundation [17] had already been popular for decades among engineers. Compared to the rigorous elastic solution, "the pile on the Winkler foundation" model simplifies the soil as the discrete springs and dashpots. Hence, the mathematical work is significantly reduced to the boundary value problem of a one-dimensional rod function. The key to implementing "the pile on the Winkler foundation" model is the assessment of the elastic and damping coefficients of the complex discrete springs. For small-strain viscoelastic problems, these parameters are mainly derived from the plane strain model [18]. By neglecting the longitudinal component, the rigorous three-dimensional viscoelastic equations (e.g., Equation (1)) can be simplified to the plane strain ones (Equation (2)). Especially for the axisymmetric cases, the circumferential component can be overlooked at the same time (Equation (3)).

$$(\lambda + G)\frac{\partial^2 u}{\partial z^2} + G\nabla^2 u = \rho\frac{\partial^2 u}{\partial t^2} \tag{1}$$

$$G\frac{\partial^2 u}{r^2\partial\theta^2} + G\frac{\partial^2 u}{\partial r^2} + G\frac{\partial u}{r\partial r} = \rho\frac{\partial^2 u}{\partial t^2} \tag{2}$$

$$G\frac{\partial^2 u}{\partial r^2} + G\frac{\partial u}{r\partial r} = \rho\frac{\partial^2 u}{\partial t^2} \tag{3}$$

where $\nabla^2 = \frac{\partial^2}{\partial z^2} + \frac{\partial^2}{r^2\partial\theta^2} + \frac{\partial^2}{\partial r^2} + \frac{\partial}{r\partial r}$; λ and G are the lame constants of the soil; u denotes the longitudinal displacement of the soil. It can be easily found that Equation (3) is a cylindrical differential function whose analytical solution can be expressed in the form of the Bessel function. Hence, the soil impedance containing the stiffness and damping can be derived [19]. In most cases, the plane strain model can be used directly instead of the Winkler model, obtaining higher calculation accuracy. For example, the complex springs in the Winkler model were put into series in the radial direction to simulate the radial inhomogeneity caused by pile installation by some scholars [20,21]. By doing this, the overall impedance of the complex springs would be smaller than any individual complex spring in the series. This can reflect the weakening of the surrounding soil after bore drilling during the installation of bored piles. In contrast, it fails to model the strengthening of the surrounding soil after the driving of precast piles. By adopting the plane strain model, the gradient soil strengthening along the radial direction can be authentically simulated by discretizing the soil into numerous circular zones and enforcing continuous boundary conditions at the interfaces of adjacent zones [22]. Figure 1 illustrates the advantages of modeling the radial inhomogeneity of the soil with the plane strain model over the Winkler model. Besides being more reliable and accessible, another advantage of applying the plane strain model to derive the elastic and damping coefficients in the Winkler model is that the plane strain model can take the inertia effect of the soil into account. The inertia effect is one of the key differences between static and dynamic equations. The utilization of the plane strain model effectively distinguishes the dynamic analysis from the static analysis. Except for the high computational efficiency, the Winkler model also has the features of good adaptivity and editability. For instance, after certain modifications, it can also model the slippage at the soil–pile interface when encountering large strain deformation [23,24].

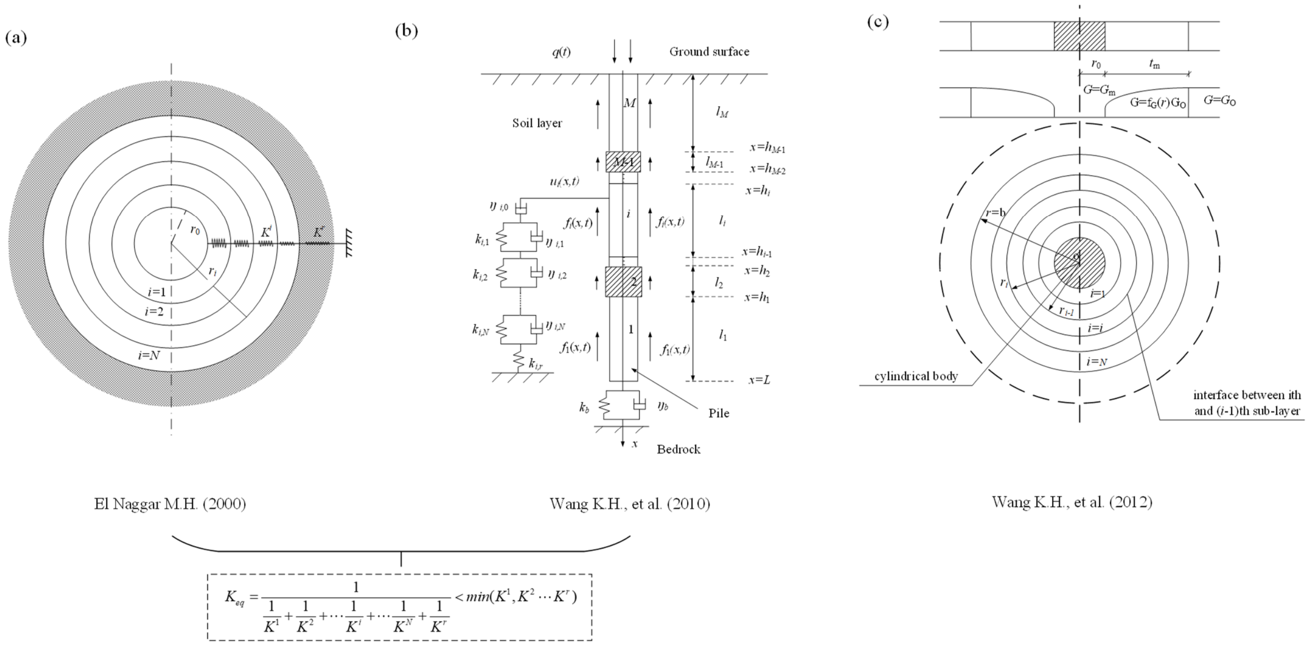

Figure 1. Advantages of plane strain model for modeling of the radial inhomogeneous problem: (**a**) tandem spring model [20]; (**b**) Voigt model in series [21]; (**c**) plane strain model [22].

However, the dynamic Winkler model is still an approximation to the rigorous answers [25]. Compared to the rigorous ones, the dynamic Winkler model has the following drawbacks:

1. Incapable of simulating the stress or strain wave propagation inside the soil.
2. Incapable of modeling the multi-phase nature of the soil.
3. Incapable of modeling the soil plug inside the pipe pile.

The derivation of some analytical solutions to the rigorous 3D continuum model enriches the knowledge of the longitudinal vibration of piles embedded in the sand, saturated marine clay, unsaturated clay, etc. The one-phase 3D continuum model is a preliminary update to the Winkler model. For most axisymmetric problems, the governing equations of the one-phase soil can be written as Equation (4).

$$\begin{cases} G\left(\nabla^2 - \frac{1}{r^2}\right)u_r + (\lambda + G)\frac{\partial e}{\partial r} = \rho\frac{\partial^2 u_r}{\partial t^2} \\ G\nabla^2 u_z + (\lambda + G)\frac{\partial e}{\partial z} = \rho\frac{\partial^2 u_z}{\partial t^2} \end{cases} \tag{4}$$

where $\nabla^2 = \frac{\partial^2}{\partial z^2} + \frac{\partial^2}{\partial r^2} + \frac{\partial}{r\partial r}$; λ and G are the lame constants of the soil; u_r and u_z denote the radial and longitudinal displacement of the soil, respectively. Nogami and Novak [26] further simplified the mathematical work by overlooking the radial displacement of the soil and derived the analytical solution to the dynamic response of a pile embedded in homogeneous anisotropic viscoelastic one-phase soil. Subsequently, it was found that the mathematical effort would not significantly increase if appropriate differential operators could be found to decouple the rigorous equations, as shown in Equation (4) [27]. With two scalar potentials (shown in Equations (5) and (6)), Senjuntichai and Rajapakse [28] decoupled Equation (4) into two Laplace functions (shown in Equations (7) and (8)) in the complex number field and derived the analytical solution to the response of a circular cavity in a semi-infinite viscoelastic medium.

$$u_{rj}(r,z) = \frac{\partial \phi_j(r,z)}{\partial r} + \frac{\partial^2 \varphi_j(r,z)}{\partial z \partial r} \tag{5}$$

$$u_{zj}(r,z) = \frac{\partial \phi_j(r,z)}{\partial z} - \frac{1}{r}\frac{\partial}{\partial r}\left(r\frac{\partial \varphi_j(r,z)}{\partial r}\right) \tag{6}$$

$$\left(\lambda_j + 2G_j\right) \cdot \nabla^2 \phi_j(r,z) = \rho s^2 \phi_j(r,z) \tag{7}$$

$$G_j \nabla^2 \varphi_j(r,z) = \rho s^2 \varphi_j(r,z) \tag{8}$$

Wu et al. [29] further investigated the influence of radial displacement of the soil on the dynamic response of the pile under axisymmetric longitudinal vibration cases. In his study, an analytical solution to the pile dynamic response utilizing mathematical techniques, including the Laplace transform, partial differential equation decoupling, variable separation, and the inverse Fourier transform, is derived. Under the same mathematical framework, studies investigating the hysteretic damping and soil plug effects were successively reported [30,31]. The necessity of employing the 3D continuum model instead of the plane strain model is that it can reveal the resonance frequencies in the low-frequency domain. As shown in Figure 2, the most rigorous solution can genuinely reveal the first and second resonance frequencies at $a \approx 0.05$ and $a \approx 0.1$. Once the radial displacement of the soil is overlooked, the first resonance frequency cannot be distinguished. As for the plane strain model, it is not capable of revealing either the first or the second resonance frequency; however, the calculated results in the higher frequency domain coincide well. The good news about the plane strain model is that the calculated results in the low-frequency domain are all slightly smaller than those calculated by rigorous 3D solutions. Hence, due to the underestimation of the pile stiffness, the stiffness decrease at the resonance frequencies is mitigated. Except for the calculation related to the resonance frequencies, the utilization of the plane strain model is biased toward safety.

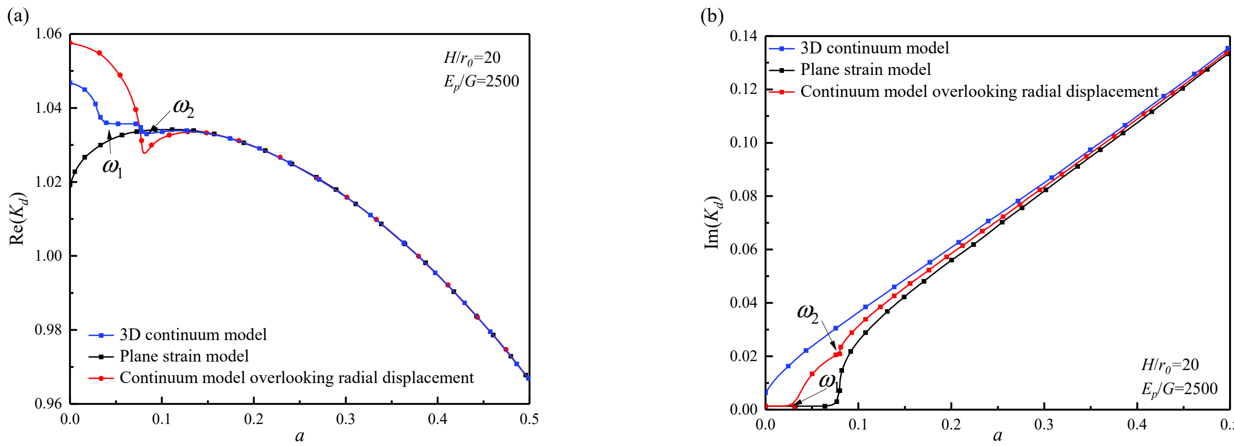

Figure 2. Pile impedance calculated by plane strain, simplified continuum model, and 3D continuum model: (**a**) dynamic stiffness; (**b**) dynamic damping (reproduced from Zheng et al. (2015) [30]).

In nature, the soil usually behaves as a multi-phase medium, whereas the above-mentioned studies all treated the soil as a solid material. As the first theory capable of coupling the solid and pore fluid inside the saturated soil, Biot's poroelastic theory is the most popular theoretical basis for poroelastic medium [32,33]. One of the most classic analytical solutions to the dynamic consolidation equations given by Biot is the displacement function method proposed by McNamee and Gibson [34]. Although Biot had established the 3D poroelastic equations for the saturated soil medium, deriving the true 3D analytical solution to the problem remains a great challenge so far. McNamee and Gibson [34] simplify the equations into the plane strain and the axisymmetric cases, which is capable of modeling almost all the horizontal and longitudinal consolidation and wave propagation problems. As the 3D problems degenerated into the plane strain and the axisymmetric problems, the utilization of the Fourier and Hankel transforms to solve the Bessel function problems became straightforward. Ai and Wang [35] derived an efficient analytical solution to the axisymmetric Biot's consolidation problem using the Hankel and Laplace transform. As for the theoretical answers to saturated soil–pile interaction, there are generally two mainstream methods: one is decoupling the 'model' [36,37], and the other one is decoupling the 'equations'. The differences between these two methods are evident. The method of decoupling the 'model' tried to reduce the soil–pile interaction problems back to the elastic problems of infinite half-space, which can be solved under the framework of Green's function. To some extent, the soil–pile interaction problems can be regarded as the response of the infinite half-space with a cylindrical area (pile) being specially strengthened. Hence, the problem can be reduced by decoupling the soil–pile interaction model into an infinite half-space and a fictitious bar, and the properties of the fictitious bar are equal to the properties of the pile minus the ones of the soil. Then, by enforcing the superposition principle in elasticity, the displacement fields of the bar (pile) and the soil are compatible. Utilizing this approach, Zeng and Rajapakse [36] investigated the influence of the nondimensional parameter b^*, which equals the fluid viscosity divided by the soil permeability, on the pile dynamic impedance. A reproduction of their findings is plotted in Figure 3. As they pointed out, b^* has a more significant influence on the damping (imaginary part of impedance) than on the stiffness (real part of impedance), and 'the poroelastic effect is more dominant in clays rather than in sands' [36]. The derivation of this method involves considerable mathematical effort, and the involvement of integral functions significantly limits the computational efficiency of the program. As for the other approach, "decoupling the equations" inherits the thought used in the derivation of one-phase soil, whose aim is to decouple the differential equations into the PDEs that have general analytical solutions. For instance, Liu et al. [38] introduced the potential functions to decouple the axisymmetric Biot's poroelastic equations. They found out that the increase in the permeability coefficients would result in larger oscillation amplitudes of both the dynamic stiffness and damping and increased resonance frequencies, as shown in Figure 4. The above-mentioned studies significantly enrich the knowledge of the dynamic saturated soil–pile interactions. However, the unsaturated soil, containing the soil skeleton, pore fluid, and air bubbles, is more prevalent in nature. It is reported that the air bubble inside the pore will generate considerable matrix suction, increasing the effective stress and stiffness of the soil [39–41]. Based on the Van Geluchten (V–G) model, Shan et al. [42] and Ye and Ai [43] established the unsaturated soil–pile dynamic interaction model, and Ma et al. [44] extended the study to the pile group case. As the saturation of soil decreases, the matrix suction becomes stronger. As a result, both the dynamic stiffness and damping increase as the saturation decreases, which is demonstrated in Figure 5. Hence, utilizing the saturated soil–pile model to investigate the pile in unsaturated soil would underestimate the dynamic impedance of the pile. To sum up, as shown in Figure 6, the theory of the longitudinal soil–pile dynamic interaction has experienced a development process from the Winkler model to the plane strain model to the three-dimensional one-phase continuum model to the multi-phase continuum model.

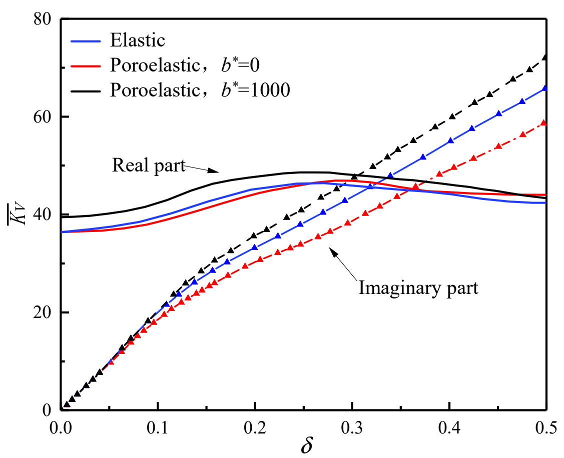

Figure 3. Influence of fluid viscosity and permeability of soil on pile impedance (reproduced from Zeng and Rajapakse (1999) [36]).

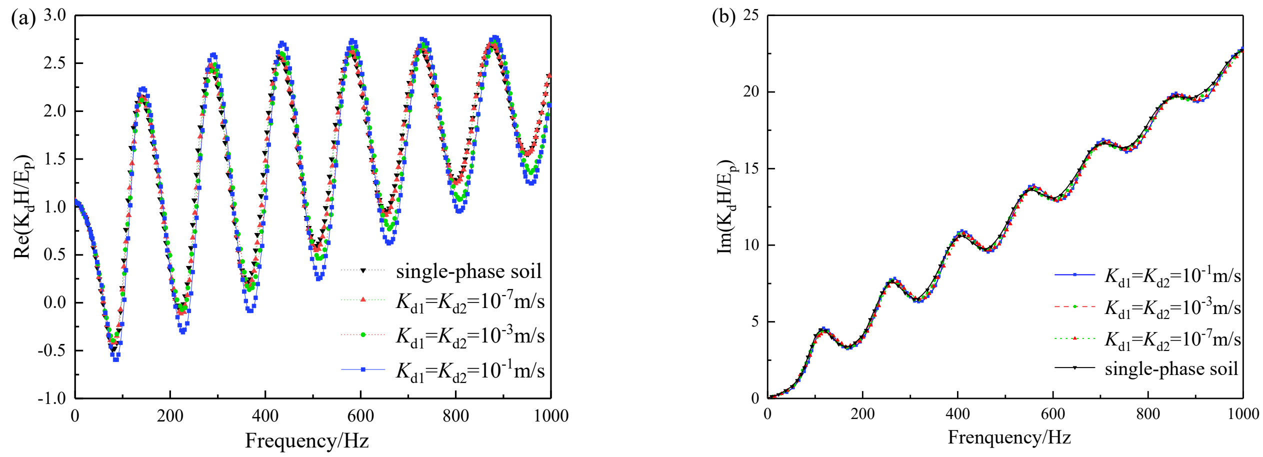

Figure 4. Influence of permeability of soil on pile impedance: (**a**) dynamic stiffness; (**b**) dynamic damping (reproduced from Liu et al. (2014) [38]).

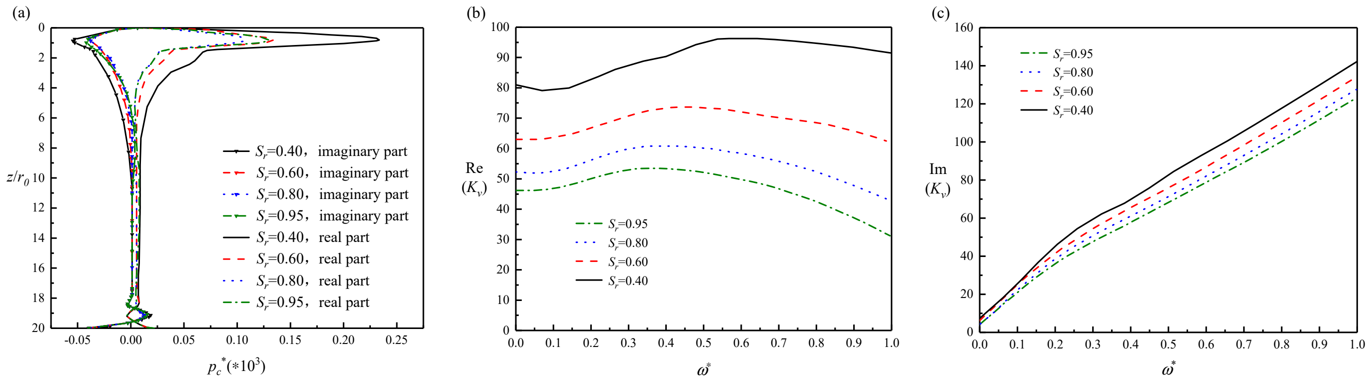

Figure 5. Influence of saturation of unsaturated soil: (**a**) matric suction; (**b**) dynamic longitudinal stiffness; (**c**) dynamic longitudinal damping (reproduced from Ye and Ai (2022) [43]).

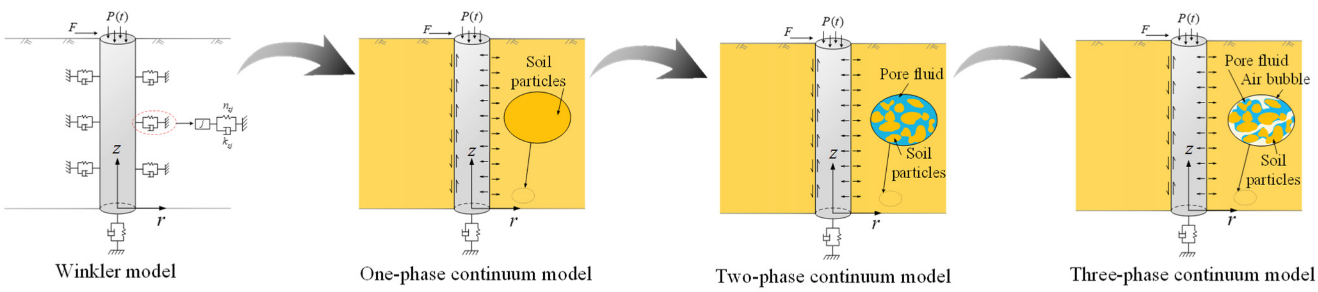

Figure 6. Development of the dynamic soil–pile interaction model.

2.2. Progress in the Pile End Soil Modeling and Its Application in Strain Wave Modeling

The strain wave propagation across the soil–pile system is an important issue in the discipline of earthquake engineering, structural dynamics, and structural health monitoring. The multi-phase continuum theory is fully capable of modeling the wave propagation inside the soil medium, whereas the reflection boundaries of the pile can significantly influence the simulation results of the wave reflection. Numerous studies have proven that the reflection of the strain wave is usually triggered by the alternation of the pile cross-section's impedance [45,46]. The most signification alternation of the impedance usually happens at the interface of the pile bottom and the soil. Hence, the reflection at the interface of the pile bottom and pile end soil is usually significant. The simplest approach to simulate this wave reflection boundary is setting the pile bottom fixed (simply regarding the displacement of the pile bottom as zero) [45–49]. The results calculated by the fixed pile bottom model [45–49] can be easily distinguished from other results, for the reflected wave shows an opposite oscillation direction compared to the incident wave. However, in practice, engineers would find that the oscillation direction of the reflected signal is usually in accordance with the incident wave. This is because, in most cases, the soil layer or bedrock at the bottom of the pile is not hard enough to prohibit the small deformations from occurring and thus usually leads to the reflected waves sharing the same direction as the incident wave. As an extension of the Boussinesq solution inside the semi-infinite medium, Mindlin [50] provided a rigorous solution to the internal stress distribution under a point load inside a semi-infinite space. On the basis of the superposition principle in linear elasticity, Poulos and Davis [51] dispersed the pile into several continuous rigid bodies and integrated the soil–rigid body interactions from the pile bottom to the pile head to calculate the overall static settlement of the pile. However, as for dynamic analysis, this rigorous answer becomes extremely mathematically sophisticated, making it only suitable for academic research [52]. In practice, the Voigt model [53,54], which uses discrete springs and dashpots to simplify the viscoelastic interaction at the pile bottom, has gained much popularity. The Voigt model is mathematically convenient and easy to implement, despite the disadvantages of vague spring and dashpot coefficients for the model. The values for the springs and dashpots in the Voigt model are generally experiment-based, and few rigorous or simplified theoretical equations have been established to assess the elastic and damping coefficients in the model. To overcome this limitation, Wu et al. [55,56] proposed the fictitious soil pile model, in which a 'fictitious soil pile' is applied at the bottom of the real pile and utilized to model the soil–pile interaction at the pile bottom. The 'fictitious soil pile' properties equal the soil's properties, avoiding the shortage of vague parameter values in the Voigt model. Subsequently, a series of the "fictitious soil pile model" was developed to consider the saturation [42,57–61] and stress diffusion [62–64] at the pile bottom. The fictitious soil pile shows excellent mathematical efficiency and acceptable accuracy, and a category of this model is summarized in Figure 7. In addition, Figure 8 compares the calculated soil stresses and displacements by the fictitious soil pile model and the rigorous elastic theory, the differences of which are within the tolerance. Because of the advantages of efficiency and simplicity, the fictitious soil pile model is subsequently introduced to many other kinds of soil–pile interaction problems, such as the soil–necking pile interactions [65,66] and the soil-stepped pile interactions [67,68].

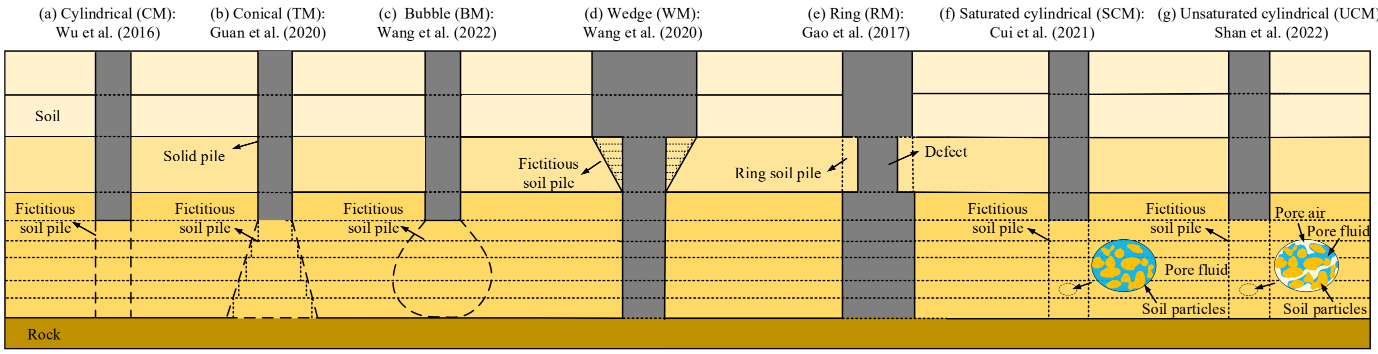

Figure 7. Category of the fictitious soil pile model: (**a**) Ref. [56]; (**b**) Ref. [63]; (**c**) Ref. [64]; (**d**) Ref. [65]; (**e**) Refs. [67,68]; (**f**) Ref. [57]; (**g**) Ref. [42].

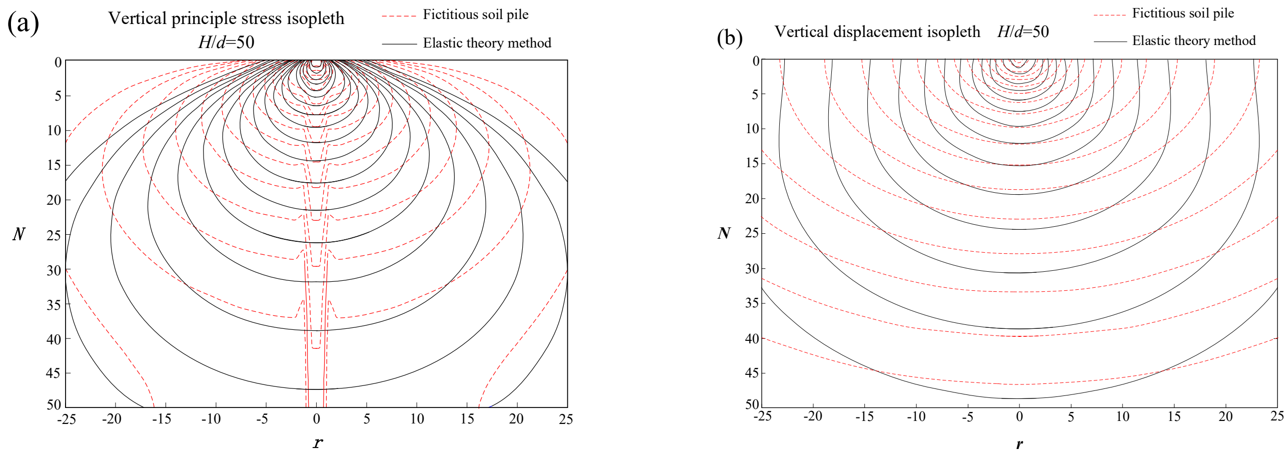

Figure 8. Stress and displacement of soil calculated by the fictitious soil pile model and the rigorous elastic theory: (**a**) principle stress; (**b**) displacement.

2.3. Progress in the 3D Soil–Pile Wave Propagation Theory

Besides the wave reflection at the pile bottom, it is found the reflection of the transverse wave at the pile shaft could be significant as the dimension of the pile increases. Many studies reported intensive interferences when conducting low-strain integrity tests for pile foundations [69–72]. The formation mechanism of this so-called "high-frequency interference" was not theoretically revealed until the last decade. The 1-D rod theory is no longer capable of revealing the "high-frequency interference" caused by transverse wave propagation. Hence, utilizing viscoelastic continuum theory, Ding et al. [73,74] established a soil–pile interaction model capable of simulating the 3D strain wave propagation inside the pipe pile. Zheng et al. [75–77] investigated the high-frequency interference under axisymmetric loading conditions, where the high-frequency interference is mainly caused by the radially propagated strain wave. Subsequently, Zheng et al. [78] extended their studies to the non-axisymmetric cases and found the high-frequency interference caused by the circumferentially propagated strain wave more significant than that caused by the radially propagated strain wave. Dai et al. [79] studied the three-dimensional wave scattering of the soil–pile system induced by the vertical P wave, and derived an analytical solution to the equivalent Winkler model for vibrations induced by the seismic P wave. Meng et al. [80] discovered that the impedance of the pile would vary radially. In detail, the most significant dynamic stiffness would appear at the center of the pipe pile, whereas the most significant dynamic damping would appear at the outer radius of the pipe pile, as shown in Figure 9. Their mathematical model also illustrates the formation mechanism of the radial transverse wave interference and the guided wave [81]. As illustrated in Figure 10, for axisymmetric loading, radially propagated Rayleigh waves induced by the incident wave would propagate between the center axis and the edge of the pile, forming high-frequency strain wave signals interfering with the signal captured at the pile head. The arrival of the incident wave at the pile head would vary significantly according to the radial positions. However, as the guided wave forms beneath the pile head, the incident strain wave would subsequently propagate in the form of a surface wave, under which circumstance the arrival of the signal starts to converge. A spectrum describing the wave propagation during non-axisymmetric loading is presented by Zhang et al. [82]. As shown in Figure 11, for non-axisymmetric loading conditions, the circumferentially propagated transverse wave dominantly governs the formation of the high-frequency interferences. The circumferentially propagated radial wave is the source of the interferences. In addition, an analogous phenomenon is observed that the differences in the arrival time of the incident wave start to mitigate as the depth increases, which is the side evidence of the formation of the guided wave. Lu et al. [83] studied the 3D wave effect of the soil–pile system under non-axisymmetric excitations and discovered that the wave signal captured at the location with 90 degrees to the excitation place is least influenced by the high-frequency interference. Based on the wave theory they established, Lu et al. [84] investigated the performance of flexural waves in identifying cracks in pipe piles. The use of continuum mechanics to model the dynamic behavior of the pile enables the reveal of high-frequency interferences. However, the mathematical complexity hinders its application in real-life engineering. Hence, in pursuit of a mathematically simpler solution, the Rayleigh–Love rod model gains popularity [85,86]. However, the original Rayleigh–Love rod model can only model the transverse inertia effect instead of the transverse wave effect. After a 3D upgrade, a modified Rayleigh–Love rod model can realize the modeling of both transverse inertia and wave effects [87]. For pipe piles, scholars also found a new engineering phenomenon, that is, the speed of stress wave propagation is closely related to the properties of the soil plug, and the higher the height of the soil plug, the smaller the wave speed [86,87]. After the work of Wu et al. [88,89], Liu et al. proposed the general additional mass model to simulate the interaction among pipe pile, soil plug, and pile surrounding soil [90], and applied the proposed model to interpret the results of low strain detection signals of pipe piles [91,92]. In order to facilitate engineers to reasonably set the test wave velocity in the low-strain detection of pipe piles, Wu et al. also proposed a new method to calculate the apparent phase velocity of open-ended pipe piles [93,94].

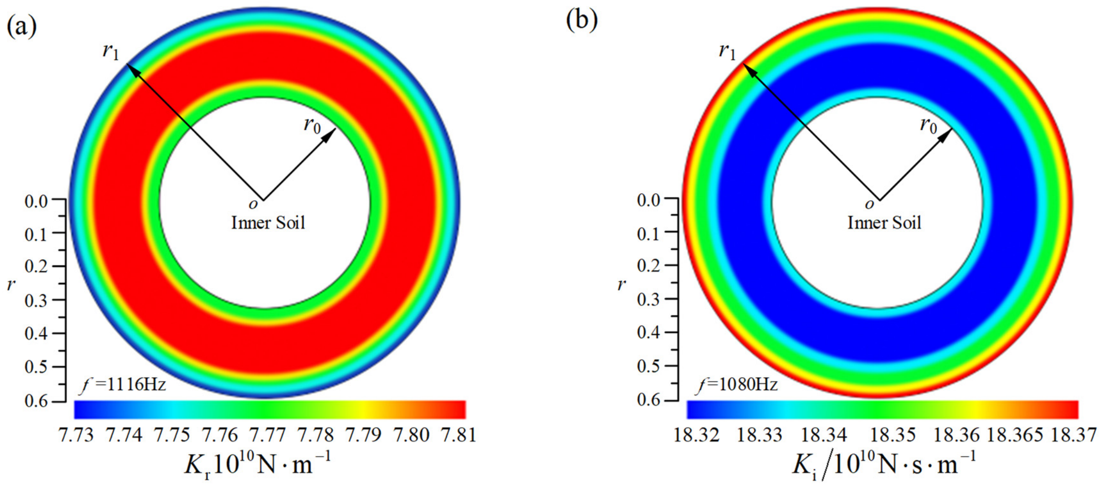

Figure 9. Variation of the pile head impedance at the cross-section of the pile (reproduced from Meng et al. (2020) [80]): (**a**) dynamic stiffness; (**b**) dynamic damping.

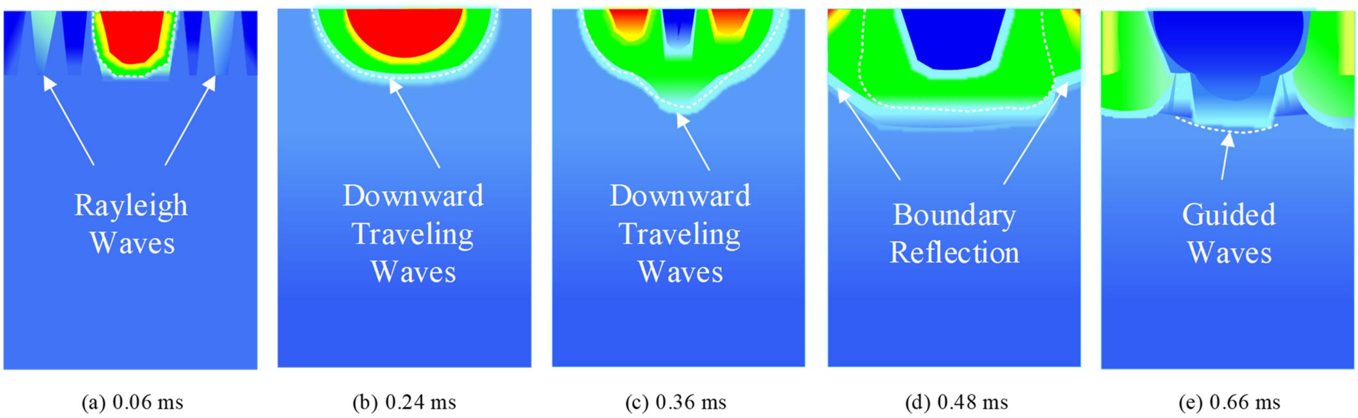

Figure 10. Formation of the high-frequency interference caused by radial transverse wave (reproduced from Meng and Su (2022) [81]).

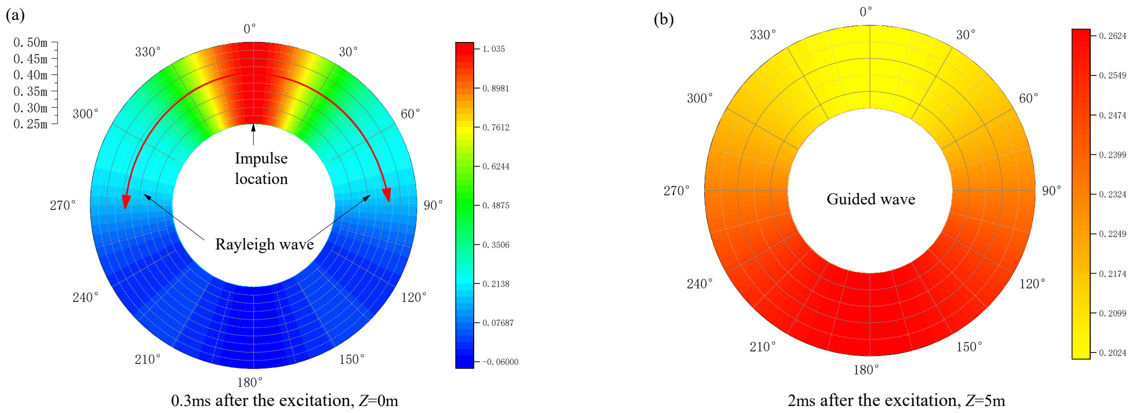

Figure 11. Formation of the high-frequency interference caused by circumferential transverse wave: (**a**) circumferentially propagated Rayleigh wave; (**b**) guided wave (reproduced from Zhang et al. (2022) [82]).

2.4. Progress in Studies Associated with the Pile Group Effect

In reality, pile foundations usually appear more in the form of pile groups, while the use of single pile foundation is quite rare [95–97]. During the vibration of pile groups, the impedance of each pile would be influenced by other piles, which is described as the "pile group effect". To account for this effect, Kaynia and Kausel [98], and Dobry and Gazetas [99] introduced the concept of 'the dynamic interaction factor α_v' to describe the relationship between the displacements of the pile induced by external loads and other pile foundations. In their model, the piles in the pile groups are classified as the active pile and passive pile: the former type of pile endures the external loads and influence the displacement of other piles, whereas the latter type of pile experience additional displacement caused by the active one. An evident defect of 'the dynamic interaction factor α_v' given by Dobry and Gazetas [99] is that it is applicable only if each pile in the pile group is subjected to equivalent external loads. To consider the 'wave diffraction' induced by different external loads, Mylonakis and Gazetas [100] utilized the Winkler model to simulate the soil–passive pile interactions. Zhang et al. [101] subsequently extended the study to the saturated soil cases. The above-mentioned 'dynamic interaction factor α_v' ignores that the additional displacement of the passive pile would, in turn, exert influence on the active pile, resulting in the additional displacement of the active pile [102]. Luan et al. [103] further took the geometry of the pile cross-section and the secondary wave effect into account and derived a more rigorous solution to the pile group response. A detailed comparison of the referred 'dynamic interaction factor α_v' is given in Table 1.

Table 1. Comparison of the referred 'dynamic interaction factor α_v' for consideration of pile group effect.

Source	Passive Pile Deformation Caused by Active Pile	Wave Diffraction Effect	Multi-Phase Nature of Soil	Active Pile Deformation Caused by Passive Pile
Kaynia and Kausel [98]	√			
Dobry and Gazetas [99]	√			
Mylonakis and Gazetas [100]	√	√		
Zhang et al. [101]	√		√	
Luan et al. [102,103]	√		√	√

3. Horizontal Dynamic Analysis and Wave Theory

3.1. General Progress in Horizontal Soil–Pile Dynamic Interaction Modeling

Horizontal dynamic analysis of pile foundations is not as common on land as longitudinal dynamic analysis. However, as the exploitation of energy develops into the deep sea, the scenarios of horizontal vibrations of the pile, for instance, offshore wind turbines and oil and gas platforms, become prevalent [104]. The dynamic Winkler model is the most popular theory utilized for the horizontal dynamic analysis of pile foundations [105–109]. Considering the implement of the dynamic Winkler model in the horizontally vibrating cases is quite similar to that in the longitudinally vibrating cases, only a brief discussion focusing on the model parameters is given. Similar to the longitudinal dynamic analysis, the elastic and damping coefficients in the Winkler model can be derived from the plane strain model [110]. Except for the plane strain model, the coefficients of the dynamic Winkler model can also be derived from the formulas given by Biot [111], Vesic [112], Klopple and Glock [113], Selvadurai [114], etc. The subgrade reactions calculated by these formulas vary significantly, and a detailed comparison of these formulas is summarized by Prendergast and Gavin [115]. It should be noted that the impedance calculated from the Winkler model can only be regarded as the initial viscoelastic complex stiffness for the subgrade reaction and can only be used for small-strain problems. For cases where the nonlinearity of the soil must be included, the *p*–*y* method can make up for the deficiencies in the nonlinear part of the soil–pile interaction. Since the scope of this review is within the viscoelastic problems, the development of the *p*–*y* method will not be discussed. However, a review of the *p*–*y* method summarized by Bouzid [116] is encouraged for reference if interested. As mentioned before, the results calculated from different elastic and damping coefficients in the Winkler model could vary significantly because many of the formulas for the coefficients in the Winkler model are either empirical or based on experimental data. Hence, the call for rigorous theoretical answers promotes the development of viscoelastic pile–soil interaction models under horizontal loads. Similar to the development of the longitudinal pile–soil dynamic interaction models, the horizontal one also experiences a developing process from the Winkler model to the simplified 3D continuum model [117,118] and then to the multi-phase 3D continuum model [119–122]. A reproduced figure, originating from Zhang et al. [119], is presented to illustrate the influence of soil saturation on the pile's dynamic horizontal impedance. As shown in Figure 12, when soil saturation increases from 0.7 to 0.999, the dynamic stiffness (real part of the impedance) could increase by 50%. In other words, the impedance of the pile could be significantly overestimated if adopting the saturated soil model to simulate the unsaturated soil. It should be noticed that this trend is opposite to that found in the longitudinal vibration situation, in which the impedance would decrease as the saturation of soil increases. For longitudinal vibrations, the utilization of the two-phase soil model is biased toward safety, whereas it turns out to be unsafe for horizontal vibrations.

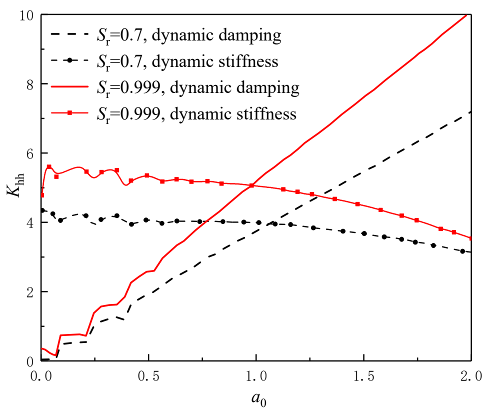

Figure 12. Influence of saturation of unsaturated soil on the dynamic horizontal impedance of the pile (reproduced from Zhang et al. (2019) [119]).

3.2. Influence of the Vertical Loads on the Horizontal Dynamic Performance of Pile

The development of the viscoelastic theory for the horizontally vibrating piles is quite similar to that of the longitudinal one: fulfillment from the Winkler model to multi-phases continuum theory, the consideration of the active and passive piles in the pile group effect, etc. Hence, in this section, some interesting findings or opposite conclusions to those drawn in longitudinal vibrations will be discussed.

One interesting phenomenon is observed when vertical loads are subjected together with the horizontal loads. According to the P-delta effect, the vertical loads would cause additional moments during the bending of the pile, whereby exacerbating the deflection of the pile. This theory is supported by several analytical studies utilizing classic Biot's poroelasticity to investigate the dynamic response of pile foundations induced by combined loads [123–125]. As one of the most representative examples, Ding et al. [123] reported that as the vertical load subjected at the pile head increases, the initial impedance decreases, and both the deflection and rotation angle would be exacerbated. However, some experimental studies as shown in Figure 13 indicated completely opposite results [126,127]. As an example, Lu and Zhang [126] conducted a model test and found that the horizontal displacement would decrease with the increase in the vertical load applied at the pile head. The theory and experiment seem to be the opposite regarding this phenomenon. Some scholars have attempted to elucidate the reasons for the differences between the theoretical and experimental results. For instance, Lu and Zhang [126] attributed this phenomenon to the strengthened pile–soil interface as the vertical load increases. Li et al. [128] thoroughly investigated the mechanics behind it and deduced that the change in the mean effective stress level could be responsible for the increased initial stiffness and capacity. However, it should be specially noted that the initial stiffness or capacity does not necessarily increase as the vertical load applied at the pile head increases. From the perspective of the authors, whether the initial impedance of the pile weakens or enhances highly relies on which effect is more significant, the P-delta effect or the enhanced pile–soil interface, and the mean effective stress level. If the P-delta effect is more dominant, the initial impedance of the pile will decrease. On the other hand, if the soil strength is significantly enhanced to overcome the adverse effect brought about by the P-delta effect, the initial impedance would increase. The slenderness ratio also plays a significant role in the results: for piles with smaller slenderness ratios, the initial impedance is more likely to increase with the increase in vertical loads applied at the pile head.

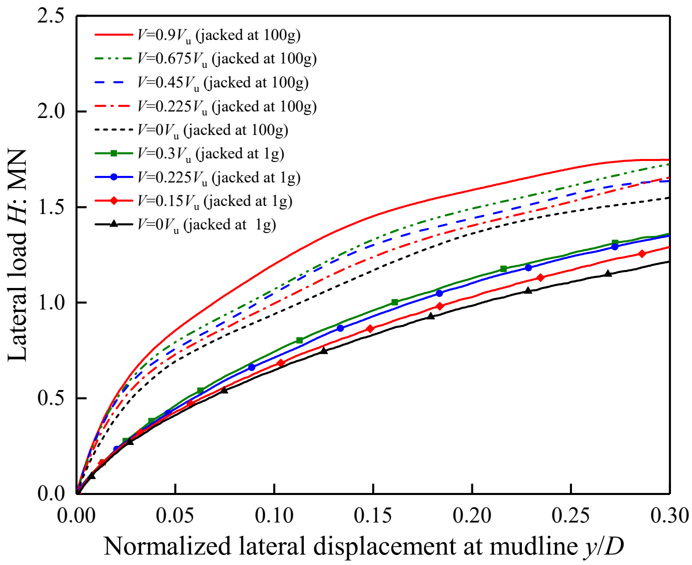

Figure 13. Influence of vertical loading on the lateral displacement of pile (reproduced from Li et al. (2022) [128]).

3.3. Progress in Coupled Soil–Pile–Water Modeling for Offshore Engineering

As lateral vibration often occurs at the pile foundations used offshore, the hydrodynamic pressure acting on the pile shaft drew the interest of the researchers. The most referred research investigating the hydrodynamic forces acting on the pile foundation came from Morison [129]. The Morison equation is the sum of two components: one is the inertia load associated with the acceleration of the wave, and the other is the drag load related to the instantaneous flow velocity. Since the inertia and dragging coefficients influence the calculated wave forces, a number of studies focus on the correction of these two coefficients [130–133]. Recently, Beji [134] extended the scope of the Morison equation by taking the geometry of the pile and the wave kinematic into consideration. Zan and Lin [135] pointed out the deficiency of the Morison equation in the internal solitary wave and proposed a modified empirical equation. Li et al. [136] further investigated the wave formulas of the interfacial periodic gravity waves in a two-layer fluid. It has already become common sense that the wave forces acting on a single pile in a pile group would increase as the gap between the piles decrease, whereas the Morison equation is not capable of modeling this phenomenon. To account for the pile group effect on wave scattering, Mindao et al. [137] introduced the interference coefficient K_g and shelter coefficient K_z to account for the wave scattering under side-by-side and tandem arrangement, respectively. Subsequently, a comprehensive study investigating the wave loads acting on the randomly arranged pile group was conducted by Bonakdar et al. [138]; the pile group effect coefficient K_G is summarized and plotted in Figure 14.

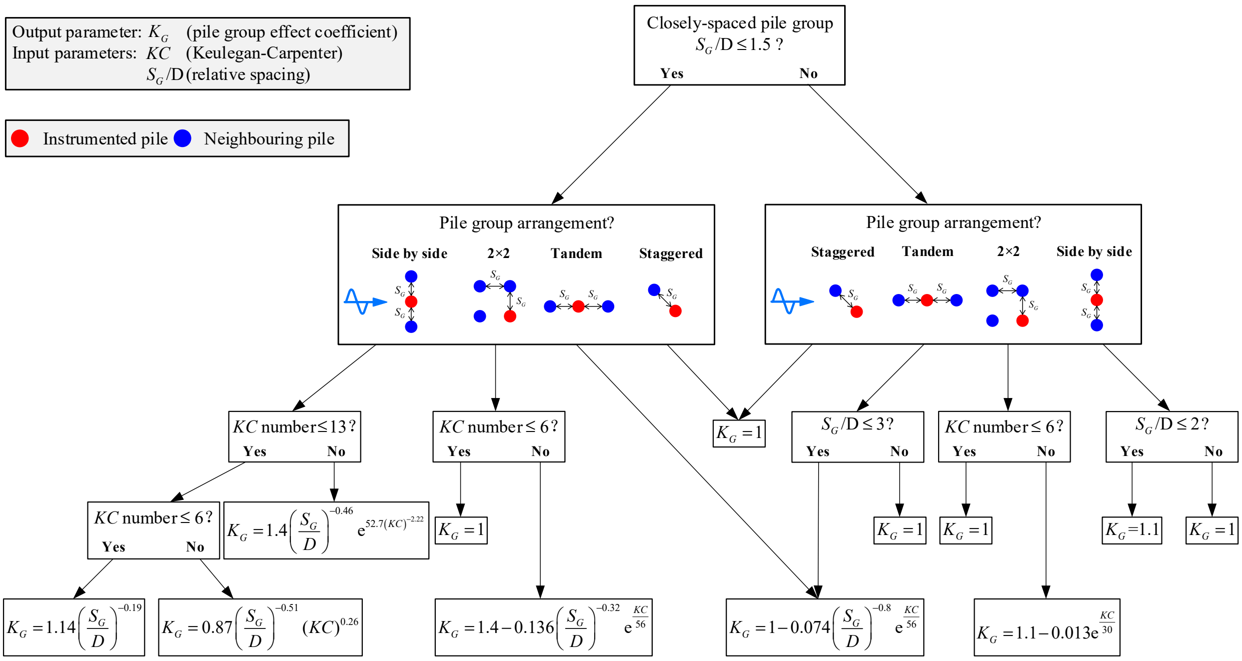

Figure 14. Pile group effect coefficients for different pile group arrangements (reproduced from Bonakdar et al. (2015) [138]).

Besides the Morison equation, the continuum equation overlooking the shear stress, which is also known as the radiation wave theory, is also a popular approach to estimating the hydrodynamic effect on pile foundation [139]. This theory originated from the hydrodynamic analysis of a dam, and was subsequently used to analysis the hydrodynamic pressure on piles [140–144]. An analytical solution to linear radiation wave theory is accessible, making it widely applied in inertia and kinematic (seismic) analysis of the laterally loaded piles [145,146]. Radiation wave theory still involves significant simplifications and is far away from a rigorous solution. Based on the Reynolds-averaged Naiver–Stokes (RANS) equations and the standard $k - \varepsilon$ model, Zhao et al. [147] established a rigorous numerical model, capable of modeling the pore pressure response caused by seawater and the consolidation during the motion. For numerical efficiency, Zhao et al. [147] utilized a quasi-static soil model instead of a dynamic soil model. To account for the inertia effect of the soil, Sui et al. [148] upgraded the model to a dynamic one and investigated the liquefication around the pile caused by the wave. The mathematical complexity hinders their application in practice, no matter the radiation wave theory or the FEM model based on RANS equations. The Morison equations or simply utilizing "added mass" to model the hydrodynamic loads remains the most popular approach in practical engineering [143,149]. It is interesting to find that most of the theories established or phenomena that happened for the lateral foundation are more suitable or prone to occur for slender piles instead of stubby piles. For instance, the Morison equation, the P-delta effect, and the plane section assumption. In fact, researchers have long found the deficiency of the Euler–Bernoulli beam (EB) theory, especially for stubby piles [150,151]. Due to the shear deformation being overlooked in the EB model, the calculated deflection could be underestimated. With the adoption of the Timoshenko beam theory, the deflection and impedance of stubby piles can be better predicted [152–154].

3.4. Progress in Seismic Performance of Pile Foundations

Compared to the dynamic loads subjected at the pile shaft, known as the inertia response, the horizontal vibrations induced by seismic loads are more significant [155–158]. Hence, numerous scholars have investigated the seismic performance of pile foundations caused by the vertically propagated S-wave. An essential simplification for the seismic response analysis in the viscoelastic medium is given by Gazetas [155], who assumed that the pile responses induced by the external loads and the seismic waves could be decomposed or superimposed. With this simplification, the horizontal seismic response of the pile foundation can be regarded as the vibrations induced by the motions of far-field soils [159]. Based on the beam-on-dynamic-Winkler foundation (BDWF) model, Torshizi et al. [160] investigated the kinematic bending strains at the pile head of the pile groups. Álamo et al. [161] studied the seismic tangential interactions between the soil and pile and verified the capability of the BDWF model by comparing it with the rigorous continuum model. The reproduced results are shown in Figure 15. As is shown, the BDWF's results are generally in accordance with the continuum model, while deviations can be observed at the soil layers' interfaces, which can be attributed to the neglect of the coordinated deformation between soil layers in the BDWF model. With the combination of the BDWF model and the finite element method (FEM), Dezi et al. [162] studied the seismic response of the pile group in layered soils.

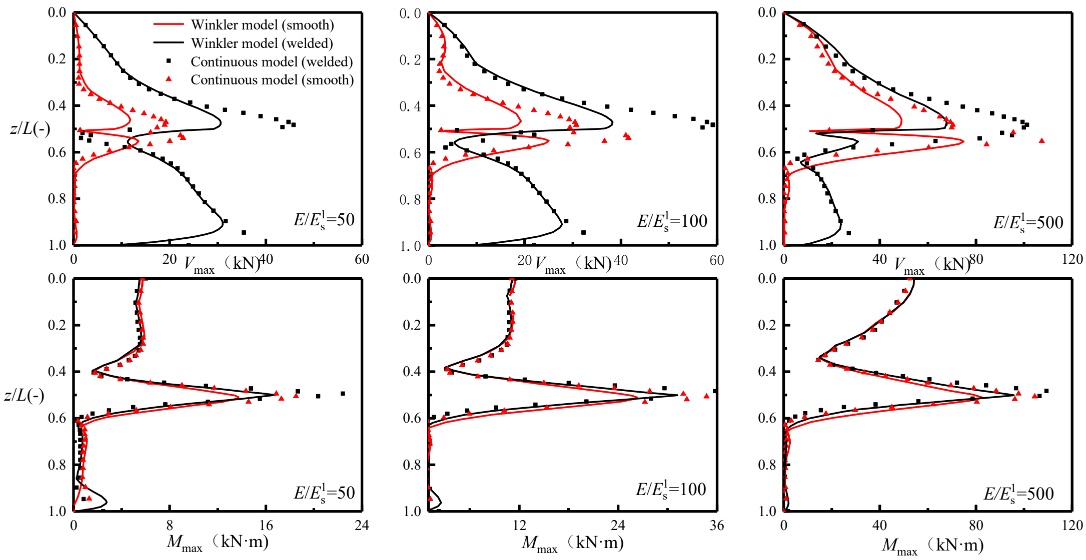

Figure 15. BDWF-based FEM results compared to the continuous model (reproduced from Álamo et al. (2018) [161]).

In pursuit of a more rigorous answer, elastic or poroelastic theories were also implemented for seismic analysis of piles in viscoelastic soil. For instance, Kaynia [163] utilized Green's function for layered media to model the dynamic response of the soil under the seismic S-wave; Zheng et al. [164] derived an analytical solution to this seismic response problem with the adoption of Biot's poroelastic equations to simulate the viscoelastic behavior of the soil; Dai et al. [165] investigated the influence of the radial inhomogeneity on the seismic response of the pile foundation. Although the acquisitions of these rigorous answers avoided the coefficients assessment in the Winkler model, they lost the simplicity, versatility, and extensibility of the Winkler model. For instance, the BDWF model can conveniently take the nonlinearity of the soil into consideration with the introduction of the *p*–*y* curve profiles of the intended soil [166], whereas the constitutive soil equations for rigorous analytical solutions are limited in linear elasticity. Usually the earthquake-induced dynamic response usually involves large strain deformation and strong nonlinearity, making these rigorous viscoelastic solutions inapplicable. To overcome the drawback that the continuity of the soil deformation is overlooked in the BDWF model, some 'two-parameter' subgrade reaction models, such as the modified Vlasov model [167–170] and the Pasternak model [171,172], are proposed by some researchers. The 'two-parameter' subgrade reaction model established the deformation relations between the adjacent springs and dashpots in the BDWF model to simulate the continuous deformation in the soil while only resulting in a limited increase in computational efforts. During the discussion of the research adopting the Winkler model, the authors pointed out that the neglect of the continuity of the spring and dashpots could cause some evident deviations at the interfaces of the soil layers compared to the continuum model, as shown in Figure 15. However, with the consideration of the continuity of the Winkler model, the deviation can be significantly reduced, as shown in Figure 16, which is a reproduction of the work by Ke et al. [170]. Although the application of FEM [173–175] or BEM [176] methods continued to expand in the soil–pile dynamic interaction problems, the BDWF model and some other subgrade reaction methods remain the most efficient and versatile ones in seismic analysis.

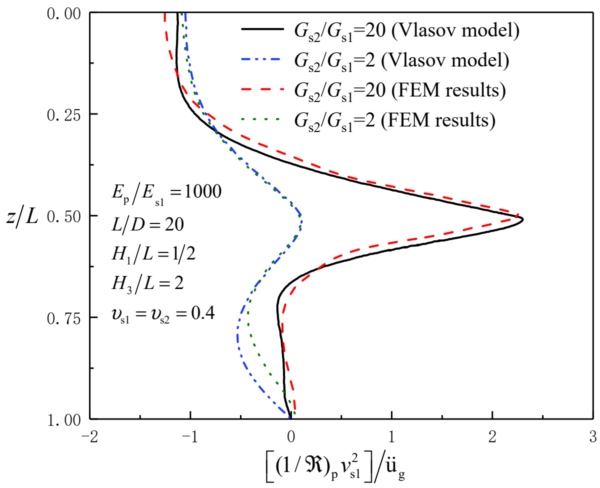

Figure 16. Results derived from the Vlasov model compared to the continuous model (reproduced from Ke et al. (2019) [170]).

4. Torsional Dynamic Analysis and Wave Theory

Compared to longitudinal and horizontal dynamic vibrations, the torsional vibration is the rarest one in practical engineering. The torsional vibration of the pile is often caused by machinery loads or unbalanced horizontal loads [177,178]. After decades of research, the torsional vibration theory of pile foundation in the viscoelastic medium had been established on the basis of the plane strain model [179–182], one-phase 3D continuum model [183–185], and multi-phase 3D continuum model [186–188], successively. For torsional vibrations, the results calculated from the plane strain model and the 3D continuum model are highly consistent, as shown in Figure 17. However, the saturation of the soil still has an unneglectable influence on the impedance of the pile. As shown in Figure 18, for a pipe pile, the saturation of the outer soil significantly influences the dynamic stiffness and damping of the pile. In detail, as the saturation of soil decreases, the dynamic stiffness of the pile would increase dramatically, whereas the dynamic damping would decrease slightly. It is also observed that the influence of the saturation of the outer soil is more pronounced than that of the inner soil. Hence, the most efficient and comparably accurate approach for torsional soil–pile modeling is adopting the multi-phase plane strain model.

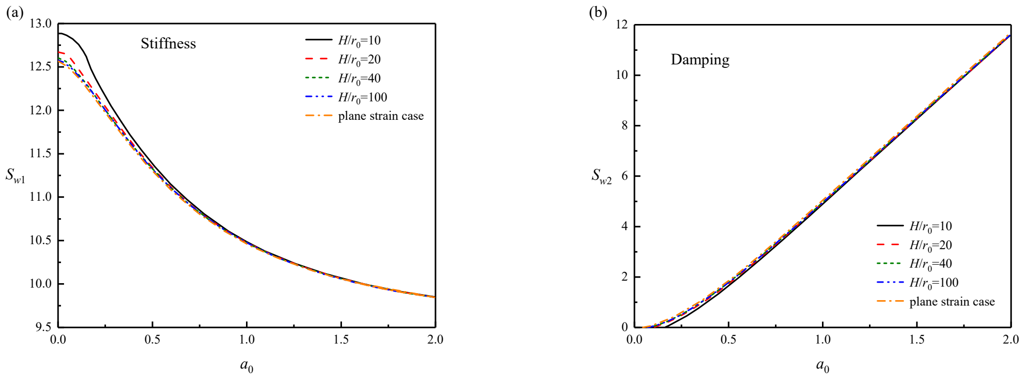

Figure 17. Comparisons between the plane strain and 3D continuum model for torsional soil–pile interaction modeling (reproduced from Wang et al. (2008) [189]): (**a**) dynamic stiffness; (**b**) dynamic damping.

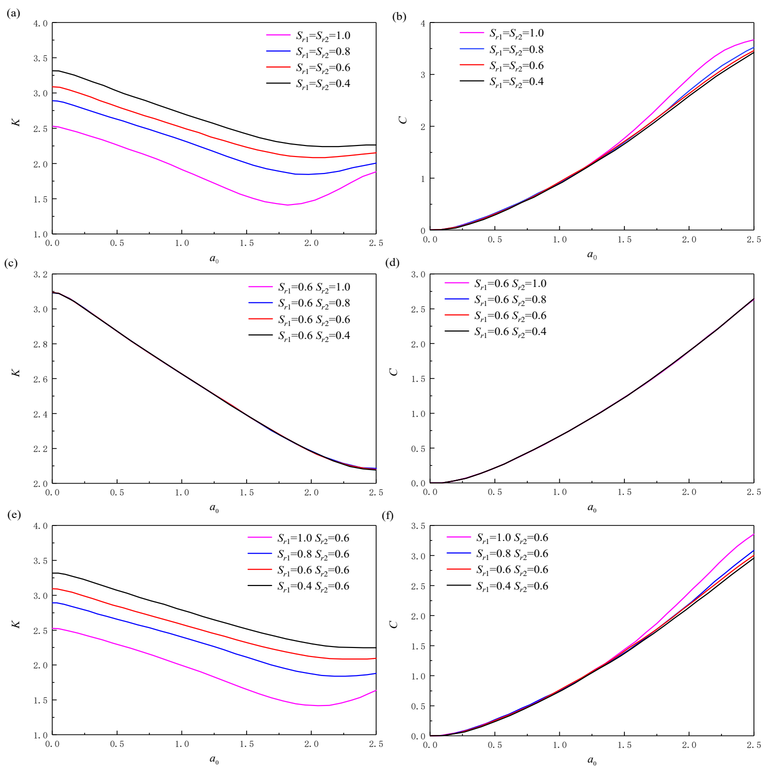

Figure 18. Influence of the saturation of soil on the dynamic torsional impedance of pile (reproduced from Ma et al. (2022) [188]): (**a**) dynamic stiffness with the variation of both the outer and inner soil's saturations; (**b**) dynamic damping with the variation of both the outer and inner soil's saturations; (**c**) dynamic stiffness with the variation of the inner soil's saturations; (**d**) dynamic stiffness with the variation of the inner soil's saturations; (**e**) dynamic stiffness with the variation of the outer soil's saturations; (**f**) dynamic damping with the variation of the outer soil's saturations.

Due to the fact that the shear wave velocity is almost half of the compressive wave velocity, some scholars pointed out that the utilization of the shear wave can effectively reduce the detection blind zone of the compressive wave if adopting the shear wave for low strain integrity test for pile foundations [190]. Considering the torsional wave signal is very rare in nature, it can hardly be interfered with by other ambient dynamic impulses, making it an optimal choice for the incident wave input. Liu et al. [191] pioneered the research of the torsional low-strain integrity test and demonstrated the advantages of having a smaller detection blind zone. Zhang et al. [192] investigated the three-dimensional torsional wave propagation and found that the high-frequency interferences during the torsional low strain integrity test are highly controllable compared to those that occurred during the longitudinal low strain integrity test. In addition, the torque can be subjected at any location of the pile shaft instead of only at the pile head, making it more versatile than the longitudinal test, especially when evaluating the existing pile foundations [193]. In summary, compared with the longitudinal wave, the torsional wave has the following advantages in structure health detection:

1. Smaller detection blind zone.
2. Less significant high-frequency interferences.
3. More versatile in existing structure health detecting.

However, it also has the following disadvantages:

1. Faster stress wave dissipation.
2. More complicated incident wave input equipment.
3. Higher requirements for sensor accuracy.

Inspired by the 3D wave effect of the torsional low strain test, it can be deduced that, for large-diameter pile foundations, the torsional impedance at the cross-section of the pile head could also vary in the radial direction. Zhang et al. [194] reported that the dimension of the pile and the differences in the elastic modulus between the inner and outer soil could significantly influence the impedance distribution across the cross-section.

5. Conclusions and Future Work

The theory of the "pile dynamics in viscoelastic medium" enables the initial impedance calculation, resonance frequency identification, and strain wave propagation modeling of the pile foundation. The calculated initial impedance and the resonance frequencies are critical parameters in the dynamic design of energy structures, while the strain wave propagation modeling is the key to the seismic response analysis and the structure health monitoring. This paper provides a state-of-the-art review of the development of longitudinal, horizontal, and torsional dynamic soil–pile interaction modeling techniques. Generally, during the decades of development, the dynamic soil–pile interaction problems within the discipline of viscoelasticity solutions are becoming more and more refined, from simplified subgrade reaction models (e.g., the Winkler, Vlasov, and Pasternak models) to rigorous multi-phase poroelastic models (e.g., the Biot's poroelastic and unsaturated soil models). For longitudinal and torsional vibration cases, the decrease in the saturation of soil shows a significantly positive influence on the dynamic impedance of the pile, indicating that the matrix suction can evidently increase the dynamic stiffness of the soil. However, for the horizontal vibration case, the decrease in the saturation of soil would decrease the dynamic impedance in the opposite case. In addition, for large diameter piles, researchers in the longitudinal and torsional vibrations both observed obvious transverse wave interference during the 3D strain wave propagation modeling, whereas the shear deformation effect was reported significant once the slenderness ratio of the pile was small during horizontal vibrations. In brief, the viscoelastic soil–pile interaction theories enable a quick and reliable calculation of the initial impedance, the deviation of which, compared to the test results, fluctuates no more than 5% in most cases [89,96].

To the best knowledge of the authors, the development of pile dynamic theories in a viscoelastic medium still has the following insufficiency. For starters, the friction and relative sliding at the soil–pile interface need further investigation since most of the present studies assumed the soil and pile maintain perfect contact during the vibrations [195]. Secondly, the effective length theory for horizontally vibrating piles needs further development. For the long piles, the entire pile length can hardly all participate in the resistance of vibrations, while only a portion of the pile length can be effective for the exerting of reactions of the foundation. Thirdly, there is a lack of research on applying the rigorous viscoelastic theory solution as the initial impedance to the nonlinear subgrade reaction solutions (e.g., p–y methods). Lastly, the theoretical answers regarding the pile group effect for torsional vibrations are scarce. For the pile group subjected to torsions, every single pile in the pile group could undergo different vibration modes, including horizontal, torsional, and superposition modes. Hence, the complexity of this problem results in very few mature theories capable of modeling this phenomenon.

Author Contributions: Conceptualization, W.W.; formal analysis, W.W. and Y.Z.; writing—original draft preparation, W.W. and Y.Z.; writing—review and editing, W.W.; supervision, W.W.; funding acquisition, W.W. All authors have read and agreed to the published version of the manuscript.

Funding: This research is supported by the National Natural Science Foundation of China (Grant No. 52178371), the Outstanding Youth Project of Natural Science Foundation of Zhejiang Province (Grant No. LR21E080005), and the Fundamental Research Founds for National University, China University of Geosciences (Wuhan) (Outstanding Ph.D. Innovation Fund, CUGDCJJ202207).

Data Availability Statement: The data presented in this study are available on request from the corresponding author.

Conflicts of Interest: The authors declare no conflict of interest.

References

1. Nguyen, C.O.; Thi, V.T.D.; Bui, D.T. Pile foundation supporting a waste water treatment reservoir in Binh Chanh soft clay. In Proceedings of the 4th International Conference on Geotechnics for Sustainable Infrastructure Development, Hanoi, Vietnam, 28–29 November 2019; Volume 62, pp. 129–135.
2. Huang, S.; Khorasanchi, M.; Herfjord, K. Drag amplification of long flexible riser models undergoing multi–mode VIV in uniform currents. *J. Fluid Struct.* **2011**, *27*, 342–353. [CrossRef]
3. Wen, K.; Gong, J.; Wu, Y. The Cascade Control of Natural Gas Pipeline Systems. *Appl. Sci.* **2019**, *9*, 481. [CrossRef]
4. Shi, Y.; Yao, W.; Yu, G. Dynamic Analysis on Pile Group Supported Offshore Wind Turbine under Wind and Wave Load. *J. Mar. Sci. Eng.* **2022**, *10*, 1024. [CrossRef]
5. Lin, Y.; Xiao, J.; Le, C.; Zhang, P.; Chen, Q.; Ding, H. Bearing Characteristics of Helical Pile Foundations for Offshore Wind Turbines in Sandy Soil. *J. Mar. Sci. Eng.* **2022**, *10*, 889. [CrossRef]
6. Chen, L.B.; Yang, X.Y.; Li, L.C.; Wu, W.B.; El Naggar, M.H.; Wang, K.J.; Chen, J.Y. Numerical Analysis of the Deformation Performance of Monopile under Wave and Current Load. *Energies* **2020**, *13*, 6431. [CrossRef]
7. Li, L.C.; Liu, X.; Liu, H.; Wu, W.B.; Lehane, B.M.; Jiang, G.S.; Xu, M.J. Experimental and numerical study on the static lateral performance of monopile and hybrid pile foundation. *Ocean Eng.* **2022**, *255*, 111461. [CrossRef]
8. Vicente, N.; José–Santos, L.G.; Dolores, E.; Pablo, A.; Mario, I.; José–María, S. Monopiles in offshore wind: Preliminary estimate of main dimensions. *Ocean Eng.* **2017**, *133*, 253–261.
9. Li, L.C.; Zheng, M.Y.; Liu, X.; Wu, W.B.; Liu, H.; El Naggar, M.H.; Jiang, G.S. Numerical analysis of the cyclic loading behavior of monopile and hybrid pile foundation. *Comput. Geotech.* **2022**, *144*, 104635. [CrossRef]
10. Kong, J.; Zhang, T.; Gui, F.; Qu, X.; Feng, D. Dynamic Response Analysis of Anchor Piles for Marine Aquaculture under Cyclic Loading. *J. Mar. Sci. Eng.* **2022**, *10*, 785. [CrossRef]
11. Xie, M.; Lopez–Querol, S. Numerical Simulations of the Monotonic and Cyclic Behaviour of Offshore Wind Turbine Monopile Foundations in Clayey Soils. *J. Mar. Sci. Eng.* **2021**, *9*, 1036. [CrossRef]
12. Cheng, X.; Wang, T.; Zhang, J.; Liu, Z.; Cheng, W. Finite element analysis of cyclic lateral responses for large diameter monopiles in clays under different loading patterns. *Comput. Geotech.* **2021**, *134*, 104104. [CrossRef]
13. Kavvadas, M.; Amorosi, A. A constitutive model for structured soils. *Géotechnique* **2000**, *50*, 263–273. [CrossRef]
14. Savvides, A.A.; Papadrakakis, M. A computational study on the uncertainty quantification of failure of clays with a modified Cam-Clay yield criterion. *SN Appl. Sci.* **2021**, *3*, 659. [CrossRef]
15. Malhotra, S. Design and Construction Considerations for Offshore Wind Turbine Foundations. In Proceedings of the ASME 26th International Conference on Offshore Mechanics and Arctic Engineering, San Diego, CA, USA, 10–15 June 2007; pp. 635–647.
16. Baranov, V.A. On the calculation of an embedded foundation. *Vorposy Din. I Progn.* **1967**, *14*, 195–209.

17. Winkler, E. *Die Lehre von der Elasticitaet und Festigkeit Mitbesondere Ruecksicht Auf Ihre Anwendung in der Technik, Fuer Polytechnische Schuhlen, Bauakademien, Ingenieure, Maschienenbauer, Architecten, etc.*; H. Dominicus: Prague, Czech Republic, 1867.
18. Anoyatis, G.; Mylonakis, G. Dynamic Winkler modulus for axially loaded piles. *Géotechnique* **2012**, *62*, 521–536. [CrossRef]
19. Novak, M. Dynamic stiffness and damping of piles. *Can. Geotech. J.* **1974**, *11*, 574–598. [CrossRef]
20. El Naggar, M.H. Vertical and torsional soil reactions for radially inhomogeneous soil layer. *Struct. Eng. Mech.* **2000**, *10*, 299–312. [CrossRef]
21. Wang, K.H.; Wu, W.B.; Zhang, Z.Q.; Leo, C.J. Vertical dynamic response of an inhomogeneous viscoelastic pile. *Comput. Geotech.* **2010**, *37*, 536–544. [CrossRef]
22. Wang, K.H.; Yang, D.Y.; Zhang, Z.Q.; Leo, C.J. A new approach for vertical impedance in radially inhomogeneous soil layer. *Int. J. Numer. Anal. Methods Geomech.* **2012**, *36*, 697–707. [CrossRef]
23. Cui, C.Y.; Meng, K.; Xu, C.S.; Wang, B.L.; Xin, Y. Vertical vibration of a floating pile considering the incomplete bonding effect of the pile–soil interface. *Comput. Geotech.* **2022**, *150*, 104894. [CrossRef]
24. Di, T.Y.; Wu, W.B.; Zhang, Y.P.; Wang, Z.Q.; Liu, X.; Xu, M.J.; Mei, G.X. Semi–analytical approach for nondestructive test for offshore pipe piles considering soil–pile slippage induced by heavy hammer impact. *Ocean Eng.* **2022**, *260*, 112080. [CrossRef]
25. Tajimi, H. Dynamic analysis of a structure embedded in an elastic stratum. In Proceedings of the 4th World Conference on Earthquake Engineering, Santiago, Chile, 13–18 January 1969; pp. 53–69.
26. Nogami, T.; Novak, M. Soil–pile interaction in vertical vibration. *Earthq. Eng. Struct. Dyn.* **1976**, *4*, 277–293. [CrossRef]
27. Rajapakse, R.K.N.D.; Shah, A.H. On the longitudinal harmonic motion of an elastic bar embedded in an elastic half-space. *Int. J. Solids Struct.* **1987**, *23*, 267–285. [CrossRef]
28. Senjuntichai, T.; Rajapakse, R.K.N.D. Transient response of a circular cavity in a poroelastic medium. *Int. J. Numer. Anal. Methods Geomech.* **1993**, *17*, 357–383. [CrossRef]
29. Wu, W.B.; Wang, K.H.; Zhang, Z.Q.; Leo, C.J. Soil–pile interaction in the pile vertical vibration considering true three–dimensional wave effect of soil. *Int. J. Numer. Anal. Methods Geomech.* **2013**, *37*, 2860–2876. [CrossRef]
30. Zheng, C.J.; Ding, X.M.; Li, P.; Fu, Q. Vertical impedance of an end–bearing pile in viscoelastic soil. *Int. J. Numer. Anal. Methods Geomech.* **2015**, *39*, 676–684. [CrossRef]
31. Zheng, C.J.; Ding, X.M.; Sun, Y.F. Vertical vibration of a pipe pile in viscoelastic soil considering the three dimensional wave effect of soil. *Int. J. Geomech.* **2015**, *16*, 04015037. [CrossRef]
32. Biot, M.A. Theory of Propagation of Elastic Waves in a Fluid–Saturated Porous Solid. I. Low–Frequency Range. *J. Acoust. Soc. Am.* **1956**, *28*, 168–178. [CrossRef]
33. Biot, M.A. Theory of Propagation of Elastic Waves in a Fluid–Saturated Porous Solid. II. Higher Frequency Range. *J. Acoust. Soc. Am.* **1956**, *28*, 179–191. [CrossRef]
34. McNamee, J.; Gibson, R.E. Displacement functions and linear transforms applied to diffusion through porous elastic media. *Q. J. Mech. Appl. Math.* **1960**, *13*, 98–111. [CrossRef]
35. Ai, Z.Y.; Wang, Q.S. A new analytical solution to axisymmetric Biot's consolidation of a finite soil layer. *J. Appl. Math. Mech.* **2008**, *29*, 1617–1624. [CrossRef]
36. Zeng, X.; Rajapakse, R.K.N.D. Dynamic axial load transfer from elastic bar to poroelastic medium. *J. Eng. Mech.* **1999**, *125*, 1048–1055. [CrossRef]
37. Senjuntichai, T.; Keawsawasvong, S.; Rajapakse, R.K.N.D. Vertical vibration of a circular foundation in a transversely isotropic poroelastic soil. *Comput. Geotech.* **2020**, *122*, 103550. [CrossRef]
38. Liu, H.L.; Zheng, C.J.; Ding, X.M.; Qin, H.Y. Vertical dynamic response of a pipe pile in saturated soil layer. *Comput. Geotech.* **2014**, *61*, 57–66. [CrossRef]
39. Santos, J.E.; Corberó, J.M.; Douglas, J. Static and dynamic behavior of a porous solid saturated by a two–phase fluid. *J. Acoust. Soc. Am.* **1990**, *87*, 1428–1438. [CrossRef]
40. Lo, W.C.; Sposito, G.; Majer, E. Low–frequency dilatational wave propagation through unsaturated porous media containing two immiscible fluids. *Transp. Porous Media* **2007**, *68*, 91–105. [CrossRef]
41. Khoei, A.R.; Mohammadnejad, T. Numerical modeling of multiphase fluid flow in deforming porous media: A comparison between two- and three-phase models for seismic analysis of earth and rockfill dams. *Comput. Geotech.* **2011**, *38*, 142–166. [CrossRef]
42. Shan, Y.; Ma, W.J.; Xiang, K.; Wang, B.L.; Zhou, S.H.; Guo, H.J. Vertical dynamic response of a floating pile in unsaturated poroelastic media based on the fictitious unsaturated soil pile model. *Appl. Math. Model.* **2022**, *109*, 209–228. [CrossRef]
43. Ye, Z.; Ai, Z.Y. Vertical dynamic response of a pile embedded in layered transversely isotropic unsaturated soils. *J. Geotech. Geoenviron. Eng.* **2022**, *148*, 04021169. [CrossRef]
44. Ma, W.J.; Shan, Y.; Xiang, K.; Wang, B.L.; Zhou, S.H. Vertical dynamic impedance of end–bearing pile groups embedded in homogeneous unsaturated soils. *Int. J. Numer. Anal. Methods Geomech.* **2022**, *46*, 1154–1176. [CrossRef]
45. Anoyatis, G.; Di Laora, R.; Mylonakis, G. Axial kinematic response of end–bearing piles to P waves. *Int. J. Numer. Anal. Methods Geomech.* **2013**, *37*, 2877–2896. [CrossRef]
46. Anoyatis, G.; Mylonakis, G.; Tsikas, A. An analytical continuum model for axially loaded end–bearing piles in inhomogeneous soil. *Int. J. Numer. Anal. Methods Geomech.* **2019**, *43*, 1162–1183. [CrossRef]

47. Anoyatis, G.; Mylonakis, G. Analytical Solution for axially loaded piles in two-layer soil. *J. Eng. Mech.* **2020**, *146*, 04020003. [CrossRef]
48. Xiao, S.; Wang, K.; Gao, L.; Wu, J. Dynamic characteristics of a large-diameter pile in saturated soil and its application. *Int. J. Numer. Anal. Methods Geomech.* **2018**, *42*, 1255–1269. [CrossRef]
49. Perić, D.; Cossel, A.E.; Sarna, S.A. Analytical solutions for thermomechanical soil structure interaction in end–bearing energy piles. *J. Geotech. Geoenviron. Eng.* **2020**, *146*, 04020047. [CrossRef]
50. Mindlin, R.D. Force at a point in the interior of a semi-infinite solid. *Physics* **1936**, *7*, 195–202. [CrossRef]
51. Poulos, H.G.; Davis, E.H. The Settlement behaviour of single axially loaded incompressible piles and piers. *Géotechnique* **1968**, *18*, 351–371. [CrossRef]
52. Suraparb, K.; Teerapong, S. Influence of anisotropic properties on vertical vibrations of circular foundation on saturated elastic layer. *Mech. Res. Commun.* **2018**, *94*, 102–109.
53. Li, Z.Y.; Wang, K.H.; Wu, W.B.; Leo, C.J.; Wang, N. Vertical vibration of a large–diameter pipe pile considering the radial inhomogeneity of soil caused by the construction disturbance effect. *Comput. Geotech.* **2017**, *85*, 90–102. [CrossRef]
54. Li, Z.Y.; Gao, Y.F. Effects of inner soil on the vertical dynamic response of a pipe pile embedded in inhomogeneous soil. *J. Sound Vib.* **2019**, *439*, 129–143. [CrossRef]
55. Wu, W.B.; Wang, K.H.; Ma, S.J.; Chin, J.L. Longitudinal dynamic response of pile in layered soil based on virtual soil pile model. *J. Cent. South Univ.* **2012**, *19*, 1999–2007. [CrossRef]
56. Wu, W.B.; Liu, H.; El Naggar, M.H.; Mei, G.X.; Jiang, G.S. Torsional dynamic response of a pile embedded in layered soil based on the fictitious soil pile model. *Comput. Geotech.* **2016**, *80*, 190–198. [CrossRef]
57. Cui, C.Y.; Meng, K.; Pei, H.F. Analytical solution for longitudinal vibration of a floating pile in saturated porous media based on a fictitious saturated soil pile model. *Comput. Geotech.* **2021**, *131*, 103942. [CrossRef]
58. Yang, X.Y.; Wang, L.X.; Wu, W.B.; Liu, H.; Jiang, G.S.; Wang, K.H.; Mei, G.X. Vertical dynamic impedance of a viscoelastic pile in arbitrarily layered soil based on the fictitious soil pile model. *Energies* **2022**, *15*, 2087. [CrossRef]
59. Meng, K.; Cui, C.; Xu, C.; Wang, B.; Xin, Y.; Liang, Z. Approach for defective floating pile embedded in layered saturated soils and application in pile integrity test. *Int. J. Numer. Anal. Methods Geomech.* **2022**, *46*, 2893–2912. [CrossRef]
60. Cai, Y.Y.; Liu, Z.H.; Li, T.B.; Wang, N. Vertical dynamic response of a pile embedded in radially inhomogeneous soil based on fictitious soil pile model. *Soil Dyn. Earthq. Eng.* **2020**, *132*, 106038. [CrossRef]
61. Wu, W.B.; Jiang, G.S.; Huang, S.G.; Leo, C.J. Vertical dynamic response of pile embedded in layered transversely isotropic soil. *Math. Probl. Eng.* **2014**, *2014*, 126916. [CrossRef]
62. Wang, N.; Wang, K.H.; Wu, W.B. Analytical model of vertical vibrations in piles for different tip boundary conditions: Parametric study and Applications. *J. Zhejiang Univ. Sci. A* **2013**, *14*, 79–93. [CrossRef]
63. Guan, W.J.; Wu, W.B.; Jiang, G.S.; Leo, C.J.; Deng, G.D. Torsional dynamic response of tapered pile considering compaction effect and stress diffusion effect. *J. Cent. South Univ.* **2020**, *27*, 3839–3851. [CrossRef]
64. Wang, L.X.; Wu, W.B.; Zhang, Y.P.; Li, L.C.; Liu, H.; El Naggar, M.H. Nonlinear analysis of single pile settlement based on stress bubble fictitious soil pile model. *Int. J. Numer. Anal. Methods Geomech.* **2022**, *46*, 1187–1204. [CrossRef]
65. Wang, N.; Le, Y.; Hu, W.T.; Fang, T.; Zhu, B.T.; Geng, D.X.; Xu, C.J. New interaction model for the annular zone of stepped piles with respect to their vertical dynamic characteristics. *Comput. Geotech.* **2020**, *117*, 103256. [CrossRef]
66. Le, Y.; Wang, N.; Hu, W.T.; Geng, D.X.; Jiang, Y.L. Torsional dynamic impedance of a stepped pile based on the wedged soil model. *Comput. Geotech.* **2020**, *128*, 103854. [CrossRef]
67. Gao, L.; Wang, K.H.; Wu, J.T.; Xiao, S.; Wang, N. Analytical solution for the dynamic response of a pile with a variable–sectioninterface in low–strain integrity testing. *J. Sound Vib.* **2017**, *395*, 328–340. [CrossRef]
68. Gao, L.; Wang, K.H.; Xiao, S.; Wu, W.B. Dynamic response of a pile considering the interaction of pile variable cross section with the surrounding layered soil. *Int. J. Numer. Anal. Methods Geomech.* **2017**, *41*, 1196–1214. [CrossRef]
69. Steinbach, J.; Vey, E. Caisson evaluation by stress wave propagation method. *J. Geotech. Eng. Div. Am. Soc. Civ. Eng.* **1975**, *101*, 361–378. [CrossRef]
70. Smith, I.M.; Chow, Y.K. Three-dimensional analysis of pile drivability. In Proceedings of the 2nd International Conference on Numerical Methods in Offshore Piling, Austin, TX, USA, 29–30 April 1982; pp. 1–20.
71. Fukuhara, T.; Kakurai, M.; Sugimoto, M. Analytical evaluation of defective piles. In Proceedings of the 14th International Conference on the Application of Stress-Wave Theory to Piles, The Hague, The Netherlands, 21–24 September 1992; pp. 563–569.
72. Chow, Y.K.; Phoon, K.K.; Chow, W.F.; Wong, K.Y. Low strain integrity testing of piles: Three–dimensional effects. *J. Geotech. Geoenviron. Eng.* **2003**, *129*, 1057–1062. [CrossRef]
73. Ding, X.M.; Liu, H.L.; Liu, J.Y.; Chen, Y.M. Wave propagation in a pipe pile for low–strain integrity testing. *J. Eng. Mech.* **2011**, *137*, 598–609. [CrossRef]
74. Ding, X.M.; Liu, H.L.; Kong, G.Q.; Zheng, C.J. Time–domain analysis of velocity waves in a pipe pile due to a transient point load. *Comput. Geotech.* **2014**, *58*, 101–116. [CrossRef]
75. Zheng, C.J.; Kouretzis, G.P.; Ding, X.M.; Liu, H.L.; Poulos, H.G. Three-dimensional effects in low-strain integrity testing of piles: Analytical solution. *Can. Geotech. J.* **2016**, *53*, 225–235. [CrossRef]
76. Zheng, C.J.; Ding, X.M.; Kouretzis, G.P.; Liu, H.L.; Sun, Y. Three-dimensional propagation of waves in piles during low–strain integrity tests. *Géotechnique* **2018**, *68*, 358–363. [CrossRef]

77. Zheng, C.J.; Kouretzis, G.P.; Ding, X.M.; Luan, L.B. Vertical vibration of end–bearing single piles in poroelastic soil considering three–dimensional soil and pile wave effects. *Comput. Geotech.* **2022**, *146*, 104740. [CrossRef]
78. Zheng, C.J.; Liu, H.L.; Ding, X.M.; Kouretzis, G.P.; Sloan, S.W.; Poulos, H.G. Non-axisymmetric response of piles in low-strain integrity testing. *Géotechnique* **2017**, *67*, 181–186. [CrossRef]
79. Dai, D.H.; El Naggar, M.H.; Zhang, N.; Gao, Y.F. Kinematic response of an end-bearing pile subjected to vertical P-wave considering the three-dimensional wave scattering. *Comput. Geotech.* **2020**, *120*, 103368. [CrossRef]
80. Meng, K.; Cui, C.Y.; Liang, Z.M.; Li, H.J.; Pei, H.F. A new approach for longitudinal vibration of a large–diameter floating pipe pile in visco-elastic soil considering the three-dimensional wave effects. *Comput. Geotech.* **2020**, *128*, 103840. [CrossRef]
81. Meng, K.; Su, H.F. Analytical model of large-diameter viscoelastic floating pile and application in pile low–strain integrity testing. *Soil Dyn. Earthq. Eng.* **2022**, *158*, 107296. [CrossRef]
82. Zhang, Y.P.; Liu, H.; Wu, W.B.; Wang, L.X.; Jiang, G.S. A 3D analytical model for distributed low strain test and parallel seismic test of pipe piles. *Ocean Eng.* **2021**, *225*, 108828. [CrossRef]
83. Lu, Z.T.; Wang, Z.L.; Liu, D.J. Study on low–strain integrity testing of pipe–pile using the elastodynamic finite integration technique. *Int. J. Numer. Anal. Methods Geomech.* **2013**, *37*, 536–550. [CrossRef]
84. Lu, Z.T.; Wang, Z.L.; Liu, D.J.; Feng, X.; Ma, H.C.; Tan, X.H. Propagation characteristics of flexural wave and the reflection from vertical cracks during pipe–pile integrity testing. *Int. J. Numer. Anal. Methods Geomech.* **2022**, *46*, 1660–1684. [CrossRef]
85. Lü, S.H.; Wang, K.H.; Wu, W.B.; Leo, C.J. Longitudinal vibration of a pile embedded in layered soil considering the transverse inertia effect of pile. *Comput. Geotech.* **2014**, *62*, 90–99. [CrossRef]
86. Banerjee, J.R.; Ananthapuvirajah, A.; Papkov, S.O. Dynamic stiffness matrix of a conical bar using the Rayleigh–Love theory with applications. *Eur. J. Mech. A Solid.* **2020**, *83*, 104020. [CrossRef]
87. Zhang, Y.P.; Di, T.Y.; El Naggar, M.H.; Wu, W.B.; Liu, H.; Jiang, G.S. Modified Rayleigh–Love rod model for 3D dynamic analysis of large–diameter thin–walled pipe pile embedded in multilayered soils. *Comput. Geotech.* **2022**, *149*, 104853. [CrossRef]
88. Wu, W.B.; El Naggar, M.H.; Abdlrahem, M.; Mei, G.X.; Wang, K.H. New interaction model for vertical dynamic response of pipe piles considering soil plug effect. *Can. Geotech. J.* **2017**, *54*, 987–1001. [CrossRef]
89. Wu, W.B.; Jiang, G.S.; Huang, S.G.; Mei, G.X.; Leo, C.J. A new analytical model to study the influence of weld on the vertical dynamic response of prestressed pipe pile. *Int. J. Numer. Anal. Methods Geomech.* **2017**, *41*, 1247–1266. [CrossRef]
90. Liu, H.; Wu, W.B.; Jiang, G.S.; El Naggar, M.H.; Mei, G.X. Influence of soil plug effect on the vertical dynamic response of large diameter pipe piles. *Ocean Eng.* **2018**, *157*, 13–25. [CrossRef]
91. Liu, H.; Wu, W.B.; Jiang, G.S.; El Naggar, M.H.; Mei, G.X.; Liang, R.Z. Benefits from using two receivers for the interpretation of low-strain integrity tests on pipe piles. *Can.Geotech. J.* **2019**, *56*, 1433–1447. [CrossRef]
92. Liu, H.; Wu, W.B.; Yang, X.Y.; Jiang, G.S.; El Naggar, M.H.; Mei, G.X.; Liang, R.Z. Detection sensitivity analysis of pipe pile defects during low-strain integrity testing. *Ocean Eng.* **2019**, *194*, 106627. [CrossRef]
93. Wu, W.B.; Liu, H.; Yang, X.Y.; Jiang, G.S.; El Naggar, M.H.; Mei, G.X.; Liang, R.Z. New method to calculate apparent phase velocity of open-ended pipe pile. *Can. Geotech. J.* **2020**, *57*, 127–138. [CrossRef]
94. Liu, H.; Wu, W.B.; Ni, X.Y.; Yang, X.Y.; Jiang, G.S.; El Naggar, M.H.; Liang, R.Z. Influence of soil mass on the vertical dynamic characteristics of pipe piles. *Comput. Geotech.* **2020**, *126*, 103730. [CrossRef]
95. Dowling, J.; Finn, W.D.L.; Taiebat, M. Load distribution in large pile groups under static and dynamic loading. *Bull. Earthq. Eng.* **2016**, *14*, 1461–1474. [CrossRef]
96. Bharathi, M.; Dubey, R.N.; Shukla, S.K. Numerical simulation of the dynamic response of batter piles and pile groups. *Bull. Earthq. Eng.* **2022**, *20*, 3239–3263. [CrossRef]
97. Qu, L.M.; Ding, X.M.; Kouretzis, G.P.; Zheng, C.J. Dynamic interaction of soil and end–bearing piles in sloping ground: Numerical simulation and analytical solution. *Comput. Geotech.* **2021**, *134*, 103917. [CrossRef]
98. Kaynia, A.M.; Kausel, E. Dynamic behaviour of pile groups. In Proceedings of the Second International Conference on Numerical Methods for Offshore Piling, Austin, TX, USA, 29–30 April 1982; pp. 509–532.
99. Dobry, R.; Gazetas, G. Simple method for dynamic stiffness and damping of floating pile groups. *Géotechnique* **1988**, *38*, 557–574. [CrossRef]
100. Mylonakis, G.; Gazetas, G. Vertical vibration and additional distress of grouped piles in layered soil. *Soils Found.* **1998**, *38*, 1–14. [CrossRef]
101. Zhang, S.P.; Cui, C.Y.; Yang, G. Vertical dynamic impedance of pile groups partially embedded in multilayered, transversely isotropic, saturated soils. *Soil Dyn. Earthq. Eng.* **2019**, *117*, 106–115. [CrossRef]
102. Luan, L.B.; Zheng, C.J.; Kouretzis, G.P.; Cao, G.W.; Zhou, H. Development of a three-dimensional soil model for the dynamic analysis of end-bearing pile groups subjected to vertical loads. *Int. J. Numer. Anal. Methods Geomech.* **2019**, *43*, 1784–1793. [CrossRef]
103. Luan, L.B.; Ding, X.M.; Cao, G.W.; Deng, X. Development of a coupled pile–to–pile interaction model for the dynamic analysis of pile groups subjected to vertical loads. *Acta Geotech.* **2020**, *15*, 3261–3269. [CrossRef]
104. Cheng, X.L.; Lu, J.Q.; Zhuang, Q.; El Naggar, M.H.; Lu, Q.; Tu, W.B. Lateral cyclic behavior of OWT tripod suction bucket foundation in clays. *Ocean Eng.* **2022**, *265*, 112635. [CrossRef]
105. Mcclelland, B.; Focht, J.A. Soil Modulus for laterally loaded piles. *J. Soil Mech. Found. Div. Am. Soc. Civ. Eng.* **1956**, *82*, 1–22. [CrossRef]

106. Nogami, T.; Otani, J.; Konagai, K.; Chen, S.L. Nonlinear soil–pile interaction model for dynamic lateral motion. *J. Geotech. Eng.* **1992**, *118*, 89–106. [CrossRef]
107. Yao, S.; Nogami, T. Lateral cyclic response of a pile in viscoelastic Winkler subgrade. *J. Eng. Mech.* **1994**, *120*, 758–775. [CrossRef]
108. El Naggar, M.H.; Novak, M. Nonlinear lateral interaction in pile dynamics. *Soil Dyn. Earthq. Eng.* **1995**, *14*, 141–157. [CrossRef]
109. Gerolymos, N.; Gazetas, G. Winkler model for lateral response of rigid caisson foundations in linear soil. *Soil Dyn. Earthq. Eng.* **2006**, *26*, 347–361. [CrossRef]
110. Novak, M.; Aboul–Ella, F.; Nogami, T. Dynamic soil reactions for plane strain case. *J. Eng. Mech. Div. Am. Soc. Civ. Eng.* **1978**, *104*, 953–959. [CrossRef]
111. Biot, M.A. Bending of an infinite beam on an elastic foundation. *J. Appl. Mech.* **1937**, *59*, A1–A7. [CrossRef]
112. Vesic, A.B. Bending of beams resting on isotropic elastic solid. *J. Soil Mech. Found. Eng.* **1961**, *87*, 35–53.
113. Okeagu, B.; Abdel-Sayed, G. Coefficients of soil reaction for buried flexible conduits. *J. Geotech. Eng.* **1984**, *110*, 908–922. [CrossRef]
114. Sadrekarimi, J.; Akbarzad, M. Comparative study of methods of determination of coefficient of subgrade reaction. *Electron. J. Geotech. Eng.* **2009**, *14*, 45–61.
115. Prendergast, L.J.; Gavin, K. A comparison of initial stiffness formulations for small–strain soil–pile dynamic Winkler modelling. *Soil Dyn. Earthq. Eng.* **2016**, *81*, 27–41. [CrossRef]
116. Bouzid, D.A. Numerical investigation of large–diameter monopiles in sands: Critical review and evaluation of both API and newly proposed p–y curves. *Int. J. Geomech.* **2018**, *18*, 04018141. [CrossRef]
117. Hu, A.F.; Fu, P.; Xia, C.Q.; Xie, K.H. Horizontal impedances of saturated soil layer with radially inhomogeneous boundary zone. *Soil Dyn. Earthq. Eng.* **2018**, *111*, 184–192. [CrossRef]
118. Liu, H.; Li, J.X.; Yang, X.Y.; Chen, L.B.; Wu, W.B.; Wen, M.J.; Jiang, M.J.; Guo, C.J. Lateral dynamic response of offshore pipe piles considering effect of superstructure. *Energies* **2022**, *15*, 6759. [CrossRef]
119. Zhang, M.; Shang, W.; Wang, X.H.; Chen, Y.F. Lateral dynamic analysis of single pile in partially saturated soil. *Eur. J. Environ. Civ. Eng.* **2019**, *23*, 1156–1177. [CrossRef]
120. Zhang, M.; Zhao, C.L.; Xu, C.J. Lateral dynamic response of pile group embedded in unsaturated soil. *Soil Dyn. Earthq. Eng.* **2021**, *142*, 106559. [CrossRef]
121. Wu, W.B.; Yang, Z.J.; Liu, X.; Zhang, Y.P.; Liu, H.; El Naggar, M.H.; Xu, M.J.; Mei, G.X. Horizontal dynamic response of pile in unsaturated soil considering its construction disturbance effect. *Ocean Eng.* **2022**, *245*, 110483. [CrossRef]
122. Yang, X.Y.; Zhang, Y.P.; Liu, H.; Fan, X.X.; Jiang, G.S.; El Naggar, M.H.; Wu, W.B.; Liu, X. Analytical solution for lateral dynamic response of pile foundation embedded in unsaturated soil. *Ocean Eng.* **2022**, *265*, 112518. [CrossRef]
123. Ding, X.M.; Luan, L.B.; Zheng, C.J.; Zhou, W. Influence of the second–order effect of axial load on lateral dynamic response of a pipe pile in saturated soil layer. *Soil Dyn. Earthq. Eng.* **2017**, *103*, 86–94. [CrossRef]
124. Zheng, C.J.; Luan, L.B.; Qin, H.Y.; Zhou, H. Horizontal dynamic response of a combined loaded large–diameter pipe pile simulated by the Timoshenko beam theory. *Int. J. Struct. Stab. Dyn.* **2020**, *20*, 2071003. [CrossRef]
125. Chen, L.B.; Wu, W.B.; Liu, H.; Hu, A.F.; Newson, T.; El Naggar, M.H.; Mei, G.X.; Xu, M.J. Analytical solution for lateral vibration of offshore pipe piles considering hydrodynamic pressure. *Comput. Geotech.* **2022**, *151*, 104926. [CrossRef]
126. Lu, W.J.; Zhang, G. Influence mechanism of vertical–horizontal combined loads on the response of a single pile in sand. *Soils Found.* **2018**, *58*, 1228–1239. [CrossRef]
127. Mu, L.; Kang, X.; Feng, K.; Huang, M.; Cao, J. Influence of vertical loads on lateral behaviour of monopiles in sand. *Eur. J. Environ. Civ. Eng.* **2018**, *22*, s286–s301. [CrossRef]
128. Li, Q.; Gavin, K.G.; Askarinejad, A.; Prendergast, L.J. Experimental and numerical investigation of the effect of vertical loading on the lateral behaviour of monopiles in sand. *Can. Geotech. J.* **2022**, *59*, 652–666. [CrossRef]
129. Morison, J.R.; Johnson, J.W.; Schaaf, S.A. The force exerted by surface waves on piles. *J. Petrol. Technol.* **1950**, *2*, 149–154. [CrossRef]
130. Chakrabarti, S.K. Hydrodynamic coefficients for a vertical tube in an array. *Appl. Ocean Res.* **1981**, *3*, 2–12. [CrossRef]
131. Chakrabarti, S.K. Inline and transverse forces on a tube array in tandem with waves. *Appl. Ocean Res.* **1982**, *4*, 25–32. [CrossRef]
132. Cai, S.Q.; Long, X.M.; Wang, S.G. Forces and torques exerted by internal solitons in shear flows on cylindrical piles. *Appl. Ocean Res.* **2008**, *30*, 72–77. [CrossRef]
133. Xie, J.S.; Jian, Y.J.; Yang, L.G. Strongly nonlinear internal soliton load on a small vertical circular cylinder in two–layer fluids. *Appl. Math. Model.* **2010**, *34*, 2089–2101. [CrossRef]
134. Beji, S. Applications of Morison's equation to circular cylinders of varying cross–sections and truncated forms. *Ocean Eng.* **2019**, *187*, 106156. [CrossRef]
135. Zan, X.X.; Lin, Z.H. On the applicability of Morison equation to force estimation induced by internal solitary wave on circular cylinder. *Ocean Eng.* **2020**, *198*, 106966. [CrossRef]
136. Li, J.Y.; Liu, Z.; Liao, S.J.; Liu, Q. Fully nonlinear interfacial periodic waves in a two–layer fluid with a rigid upper boundary and their loads on a cylindrical pile. *Ocean Eng.* **2022**, *260*, 112014. [CrossRef]
137. Mindao, G.; Lihua, H.; Shaoshu, S. Experimental study for the wave forces on pile groups due to regular waves. In Proceedings of the 2nd International Conference on Coastal and Port Engineering in Developing Countries (COPEDEC), Beijing, China, 7–11 September 1987; pp. 1956–1965.
138. Bonakdar, L.; Oumeraci, H.; Etemad-Shahidi, A. Wave load formulae for prediction of wave–induced forces on a slender pile within pile groups. *Coast. Eng.* **2015**, *102*, 49–68. [CrossRef]

139. Liaw, C.Y.; Chopra, A.K. Dynamics of towers surrounded by water. *Earthq. Eng. Struct. Dyn.* **1974**, *3*, 33–49. [CrossRef]
140. Sun, K.; Nogami, T. Earthquake induced hydrodynamic pressure on axisymmetric offshore structures. *Earthq. Eng. Struct. Dyn.* **1991**, *20*, 429–440. [CrossRef]
141. Du, X.L.; Wang, P.G.; Zhao, M. Simplified formula of hydrodynamic pressure on circular bridge piers in the time domain. *Ocean Eng.* **2014**, *85*, 44–53. [CrossRef]
142. Fu, P.; Xie, K. Lateral vibration of offshore piles considering pile-water interaction. *Int. J. Struct. Stab. Dyn.* **2019**, *19*, 1950147. [CrossRef]
143. Wang, P.G.; Zhao, M.; Du, X.L. Analytical solution and simplified formula for earthquake induced hydrodynamic pressure on elliptical hollow cylinders in water. *Ocean Eng.* **2018**, *148*, 149–160. [CrossRef]
144. Chen, L.B.; Wu, W.B.; Liu, H.; El Naggar, M.H.; Wen, M.J.; Wang, K.H. Influence of defects on the lateral dynamic characteristics of offshore piles considering hydrodynamic pressure. *Ocean Eng.* **2022**, *260*, 111894. [CrossRef]
145. Huang, Y.M.; Wang, P.G.; Zhao, M.; Zhang, C.; Du, X.L. Dynamic responses of an end–bearing pile subjected to horizontal earthquakes considering water–pile–soil interactions. *Ocean Eng.* **2022**, *238*, 109726. [CrossRef]
146. Chen, L.B.; Li, J.X.; Wu, W.B.; Liu, H.; Yao, Y.; Zhang, P. New method to calculate the kinematic response of offshore pipe piles under seismic S-waves. *Soil Dyn. Earthq. Eng.* **2023**, *165*, 107651. [CrossRef]
147. Zhao, H.Y.; Jeng, D.S.; Liao, C.C.; Zhu, J.F. Three-dimensional modeling of wave-induced residual seabed response around a mono–pile foundation. *Coast. Eng.* **2017**, *128*, 1–21. [CrossRef]
148. Sui, T.T.; Zhang, C.; Jeng, D.S.; Guo, Y.K.; Zheng, J.H.; Zhang, W.; Shi, J. Wave-induced seabed residual response and liquefaction around a monopile foundation with various embedded depth. *Ocean Eng.* **2019**, *173*, 157–173. [CrossRef]
149. Wang, P.G.; Zhao, M.; Du, X.L.; Liu, J.B.; Xu, C.S. Wind, wave and earthquake responses of offshore wind turbine on monopile foundation in clay. *Soil Dyn. Earthq. Eng.* **2018**, *113*, 47–57. [CrossRef]
150. Timoshenko, S.P. On the correction for shear of the differential equation for transverse vibration of prismatic bars. *Lond. Edinb. Dubl. Phil. Mag* **1921**, *41*, 744–746. [CrossRef]
151. Kaneko, T. On Timoshenko's correction for shear in vibrating beams. *J. Phys. D Appl. Phys.* **1975**, *8*, 1927–1936. [CrossRef]
152. Wu, J.T.; El Naggar, M.H.; Wang, K.H.; Wu, W.B. Lateral vibration characteristics of an extended pile shaft under low–strain integrity test. *Soil Dyn. Earthq. Eng.* **2019**, *126*, 105812. [CrossRef]
153. Wu, T.; Sun, H.L.; Cai, Y.Q.; Wu, J.T.; Zhang, Y.P. Analytical study on the dynamic responses of a sheet–pile groin subjected to transient lateral impulses. *Ocean Eng.* **2022**, *249*, 110875. [CrossRef]
154. Wu, T.; Sun, H.L.; Aires, R.G.; Cai, Y.Q.; Wu, J.T.; Zhang, Y.P. Analytical solution for sheet–pile groin vibrations under tidal bore excitation. *Mar. Georesour. Geotechnol.* **2022**, 1–16. [CrossRef]
155. Gazetas, G. Seismic response of end-bearing single piles. *Soil Dyn. Earthq. Eng.* **1984**, *3*, 82–93. [CrossRef]
156. Yang, Z.J.; Wu, W.B.; Liu, H.; Zhang, Y.P.; Liang, R.Z. Flexible support of a pile embedded in unsaturated soil under Rayleigh waves. *Earthq. Eng. Struct. Dyn.* **2022**, *52*, 226–247. [CrossRef]
157. Yang, Z.J.; Zhang, Y.P.; Wen, M.J.; Wu, W.B.; Liu, H. Dynamic response of pile embedded in unsaturated soil under SH waves considering effect of superstructure. *J. Sound Vib.* **2022**, *541*, 117278. [CrossRef]
158. Yang, X.Y.; Jiang, G.S.; Liu, H.; Wu, W.B.; Mei, G.X.; Yang, Z.J. Horizontal dynamic response of tapered pile in arbitrary layered soil. *Energies* **2022**, *15*, 3193. [CrossRef]
159. Dong, R.; Shan, Z.D.; Jing, L.P.; Xie, Z.N.; Yin, Z.Y.; Zheng, T. Rigorous solution for kinematic response of end–bearing pile under vertically incident P-waves. *Comput. Geotech.* **2022**, *150*, 104896. [CrossRef]
160. Torshizi, M.F.; Saitoh, M.; Álamo, G.M.; Goit, C.S. Influence of pile radius on the pile head kinematic bending strains of end–bearing pile groups. *Soil Dyn. Earthq. Eng.* **2018**, *105*, 184–203. [CrossRef]
161. Álamo, G.M.; Bordón, J.D.R.; Aznárez, J.J.; Maeso, O. Relevance of soil–pile tangential tractions for the estimation of kinematic seismic forces: Formulation and setting of a Winkler approach. *Appl. Math. Model.* **2018**, *59*, 1–19. [CrossRef]
162. Dezi, F.; Carbonari, S.; Leoni, G. A model for the 3D kinematic interaction analysis of pile groups in layered soils. *Earthq. Eng. Struct. Dyn.* **2009**, *38*, 1281–1305. [CrossRef]
163. Kaynia, A.M.; Kausel, E. Dynamics of piles and pile groups in layered soil media. *Soil Dyn. Earthq. Eng.* **1991**, *10*, 386–401. [CrossRef]
164. Zheng, C.J.; Luo, T.; Kouretzis, G.; Ding, X.M.; Luan, L.B. Transverse seismic response of end–bearing pipe piles to S–waves. *Int. J. Numer. Anal. Methods Geomech.* **2022**, *46*, 1919–1940. [CrossRef]
165. Dai, D.H.; Zhang, Y.J.; Zhang, Y.F.; Wang, Z.B.; Li, Z.Y. Kinematic response of end–bearing piles under the excitation of vertical p–waves considering the construction effect. *Appl. Sci.* **2022**, *12*, 3468. [CrossRef]
166. El Naggar, M.H.; Shayanfar, M.A.; Kimiaei, M.; Aghakouchak, A.A. Simplified BNWF model for nonlinear seismic response analysis of offshore piles with nonlinear input ground motion analysis. *Can. Geotech. J.* **2005**, *42*, 365–380. [CrossRef]
167. Vallabhan, C.V.G.; Das, Y.C. Modified Vlasov model for beams on elastic foundations. *J. Geotech. Eng.* **1991**, *117*, 956–966. [CrossRef]
168. Laora, R.D.; Rovithis, E. Kinematic bending of fixed–head piles in nonhomogeneous soil. *J. Geotech. Geoenviron. Eng.* **2015**, *141*, 04014126. [CrossRef]
169. Liu, Q.J.; Deng, F.J.; He, Y.B. Transverse seismic kinematics of single piles by a modified Vlasov model. *Int. J. Numer. Anal. Methods Geomech.* **2014**, *38*, 1953–1968. [CrossRef]

170. Ke, W.H.; Liu, Q.J.; Zhang, C. Kinematic bending of single piles in layered soil. *Acta Geotech.* **2019**, *14*, 101–110. [CrossRef]
171. Filipich, C.P.; Rosales, M.B. A further study about the behaviour of foundation piles and beams in a Winkler-Pasternak soil. *Int. J. Mech. Sci.* **2002**, *44*, 21–36. [CrossRef]
172. Ke, W.; Zhang, C. A closed–form solution for kinematic bending of end–bearing piles. *Soil Dyn. Earthq. Eng.* **2017**, *103*, 15–20. [CrossRef]
173. Di Laora, R.; Mandolini, A.; Mylonakis, G. Insight on kinematic bending of flexible piles in layered soil. *Soil Dyn. Earthq. Eng.* **2012**, *43*, 309–322. [CrossRef]
174. Mucciacciaro, M.; Sica, S. Nonlinear soil and pile behaviour on kinematic bending response of flexible piles. *Soil Dyn. Earthq. Eng.* **2018**, *107*, 195–213. [CrossRef]
175. Maheshwari, B.K.; Truman, K.Z.; El Naggar, M.H.; Gould, P.L. Three–dimensional finite element nonlinear dynamic analysis of pile groups for lateral transient and seismic excitations. *Can. Geotech. J.* **2004**, *41*, 118–133. [CrossRef]
176. Stacul, S.; Squeglia, N. Simplified assessment of pile–head kinematic demand in layered soil. *Soil Dyn. Earthq. Eng.* **2020**, *130*, 105975. [CrossRef]
177. Li, Z.Y.; Gao, Y.F. Torsional vibration of a large-diameter pipe pile embedded in inhomogeneous soil. *Ocean Eng.* **2019**, *172*, 737–758. [CrossRef]
178. Zhou, H.; Yuan, J.; Liu, H. A general analytical solution for lateral soil response of non–circular cross–sectional pile segment. *Appl. Math. Model.* **2019**, *71*, 601–631. [CrossRef]
179. Novak, M.; Howell, J.F. Torsional vibration of pile foundations. *J. Geotech. Eng.* **1977**, *103*, 271–285. [CrossRef]
180. Wu, W.B.; Jiang, G.S.; Lü, S.H.; Huang, S.G.; Xie, B.H. Torsional dynamic impedance of a tapered pile considering its construction disturbance effect. *Mar. Georesour. Geotec.* **2016**, *34*, 321–330. [CrossRef]
181. Liu, H.; Jiang, G.S.; El Naggar, M.H.; Wu, W.B.; Mei, G.X.; Liang, R.Z. Influence of soil plug effect on the torsional dynamic response of a pipe pile. *J. Sound Vib.* **2017**, *410*, 231–248. [CrossRef]
182. Zhang, Y.P.; Yang, X.Y.; Wu, W.B.; El Naggar, M.H.; Jiang, G.S.; Liang, R.Z. Torsional complex impedance of pipe pile considering pile installation and soil plug effect. *Soil Dyn. Earthq. Eng.* **2020**, *131*, 106010. [CrossRef]
183. Cai, Y.Q.; Chen, G.; Xu, C.J.; Wu, D.Z. Torsional response of pile embedded in a poroelastic medium. *Soil Dyn. Earthq. Eng.* **2006**, *26*, 1143–1148. [CrossRef]
184. Zhang, Y.P.; Liu, H.; Wu, W.B.; Wang, S.; Wu, T.; Wen, M.J.; Jiang, G.S.; Mei, G.X. Interaction model for torsional dynamic response of thin-wall pipe piles embedded in both vertically and radially inhomogeneous soil. *Int. J. Geomech.* **2021**, *21*, 04021185. [CrossRef]
185. Li, Z.Y.; Gao, Y.F. Influence of the inner soil on the torsional vibration of a pipe pile considering the construction disturbance. *Acta Geotech.* **2021**, *16*, 3647–3665. [CrossRef]
186. Wang, K.H.; Zhang, Z.Q.; Leo, C.J.; Xie, K.H. Dynamic torsional response of an end bearing pile in transversely isotropic saturated soil. *J. Sound Vib.* **2009**, *327*, 440–453. [CrossRef]
187. Liu, K.F.; Zhang, Z.Q. Dynamic response of an inhomogeneous elastic pile in a multilayered saturated soil to transient torsional load. *Math. Probl. Eng.* **2021**, *2021*, 5528237. [CrossRef]
188. Ma, W.J.; Shan, Y.; Xiang, K.; Wang, B.L.; Zhou, S.H. Torsional dynamic response of a pipe pile in homogeneous unsaturated soils. *Comput. Geotech.* **2022**, *143*, 104607. [CrossRef]
189. Wang, K.H.; Zhang, Z.Q.; Leo, C.J.; Xie, K.H. Dynamic torsional response of an end bearing pile in saturated poroelastic medium. *Comput. Geotech.* **2008**, *35*, 450–458. [CrossRef]
190. Zhang, Y.P.; Jiang, G.S.; Wu, W.B.; El Naggar, M.H.; Liu, H.; Wen, M.J.; Wang, K.H. Analytical solution for distributed torsional low strain integrity test for pipe pile. *Int. J. Numer. Anal. Methods Geomech.* **2021**, *46*, 47–67. [CrossRef]
191. Liu, D.J.; Liu, Y.Z.; Wang, J.Y. Theoretical study on torsional wave applied in low strain dynamic testing of piles. *Chin. J. Geotech. Eng.* **2003**, *25*, 283–287. (In Chinese)
192. Zhang, Y.P.; Wang, Z.Q.; El Naggar, M.H.; Wu, W.B.; Wang, L.X.; Jiang, G.S. Three-dimensional wave propagation in a solid pile during torsional low strain integrity test. *Int. J. Numer. Anal. Methods Geomech.* **2022**, *46*, 2398–2411. [CrossRef]
193. Zhang, Y.P.; El Naggar, M.H.; Wu, W.B.; Wang, Z.Q. Torsional low-strain test for nondestructive integrity examination of existing high-pile foundation. *Sensors* **2022**, *22*, 5330. [CrossRef]
194. Zhang, Y.P.; El Naggar, M.H.; Wu, W.B.; Wang, Z.Q.; Yang, X.Y.; Jiang, G.S. Dynamic torsional impedance of large-diameter pipe pile for offshore engineering: 3D analytical solution. *Appl. Math. Model.* **2022**, *111*, 664–680. [CrossRef]
195. Wu, W.B.; Wang, Z.Q.; Zhang, Y.P.; El Naggar, M.H.; Wu, W.; Wen, W.J. Semi-analytical solution for negative skin friction development on deep foundations in coastal reclamation areas. *Int. J. Mech. Sci.* **2022**, *241*, 107981. [CrossRef]